NILU
TEKNISK NOTAT NR 12/78
DATE: OCTOBER 1978

ATMOSPHERIC DISPERSION EXPERIMENTS USING THE NILU AUTOMATIC WEATHER STATION AND SF_6 TRACER TECHNIQUES

BY

BRIAN LAMB AND BJARNE SIVERTSEN

NILU

NORSK INSTITUTT FOR LUFTFORSKNING

Postboks 130 - 2001 Lillestrøm

NILU
TEKNISK NOTAT NR 12/78
DATE: OCTOBER 1978

ATMOSPHERIC DISPERSION EXPERIMENTS USING THE NILU AUTOMATIC WEATHER STATION AND SF_6 TRACER TECHNIQUES

BY

BRIAN LAMB AND BJARNE SIVERTSEN

NORWEGIAN INSTITUTE FOR AIR RESEARCH
P.O. Box 130, N-2001 LILLESTRØM
NORWAY

ISBN 82-7247-088-8

LIST OF CONTENTS

ATMOSPHERIC DISPERSION EXPERIMENTS USING THE NILU AUTOMATIC WEATHER STATION AND SF_6 TRACER TECHNIQUES

1 INTRODUCTION

When applying Gaussian type dispersion models, which for many purposes might represent a useful tool in estimating air pollution concentrations, the results are sensitive to the choice of dispersion parameters. The so-called Pasquill-Gifford-Turner (PGT) curves for σ_y and σ_z (1) have been used, and misused, for about 17 years. It has been pointed out that the PGT curves apply to a sampling time of about 3 minutes, a surface roughness of a few centimeters and a latitude of about 50° (2). The selection of a proper σ-curve has been based upon atmospheric stability classes determined from observations of cloud cover and wind speed or temperature change with height (3). The dispersion class specifies both lateral and vertical spread. During the last few years several authors have emphasized the importance of estimating the lateral and vertical dispersion parameters seperately. (4,5) The use of this "split sigma" method has been demonstrated to be most important during low wind speed inversion conditions (6). To improve plume calculations, it has been recommended to estimate σ_y from measurements of lateral turbulent velocity fluctuations σ_y, or from the standard deviation of wind direction fluctuations σ_θ, and σ_z from estimates of the vertical heat flux rather than from PGT curves (7).

The purpose of this work was to validate meteorological estimates of σ_y and σ_z by using atmospheric tracer techniques. Dispersion experiments were carried out at 3 sites, using sulfur hexafluoride (SF_6) as a tracer. Meteorological data were obtained with a NILU Automatic Weather Station. This report, which summarizes the experimental tracer procedures and data handling methods, serves as a demonstration of NILU's tracer capabilities.

2 EXPERIMENTAL PROCEDURES

2.1 The NILU Automatic Weather Station (AWS)

An electronic monitor for measuring meteorological parameters including wind statistics, developed and tested at the Norwegian Institute for Air Research (NILU) (8), was used to collect dispersion data. This automatic weather station is completely digitized and has a capacity of 2 months unattended operation.

The station consists of:

1) Meteorological sensors mounted at different levels on a mast (usually 2,10,25 and 36 m).
2) An electronic unit and a datalogger placed in a small cabin or another type of shelter. The datalogger is connected to the sensors with a shielded cable normally not longer than 50 m.

The following parameters are normally logged:

Parameter	Type	Range	Resolution
1. Wind direction	Slowly averaging	0-360°	1.4°
2. Standard deviation	r.m.s. of wind direction	0-105°	1.4°
3. Wind speed	Windway	0-80 m/s	0.1 m/s
4. Wind speed gusts	Highest 10 sec average (variable average time)	0.80 m/s	0.4 m/s
5. Temperature	1000 Ω platinum	-50°C to+40°C	0.1°C
6. Temperature difference	2x1000 Ω platinum	-20°C to+20°C	0.05°C

Relative humidity, pressure or radiation may also be logged.

The datalogger is a modified Aanderaa logger. The main differences are the electronic sampling of the wind direction and its standard

deviation, extended tape capacity, digital timer with display, electronic logging of the hour number, and digital data monitor with display for direct readout of the input data. Wind direction fluctuations are measured by a windvane with damping ratio 0.6 and distance constant 1.7 meter. The AWS is shown in Figure 1. All parameter inputs are scanned every 5 minutes by the data-logger and the information is recorded in 10 bits binary code on magnetic tape.

Resolution of the logger is 250 μV which gives a total input range of 0250 mV.

Normal inspection frequency is 2 months with exchange of magnetic tape and general overhaul of the equipment. The tapes are played back at NILU and converted to IBM compatible computer tape for further data handling.

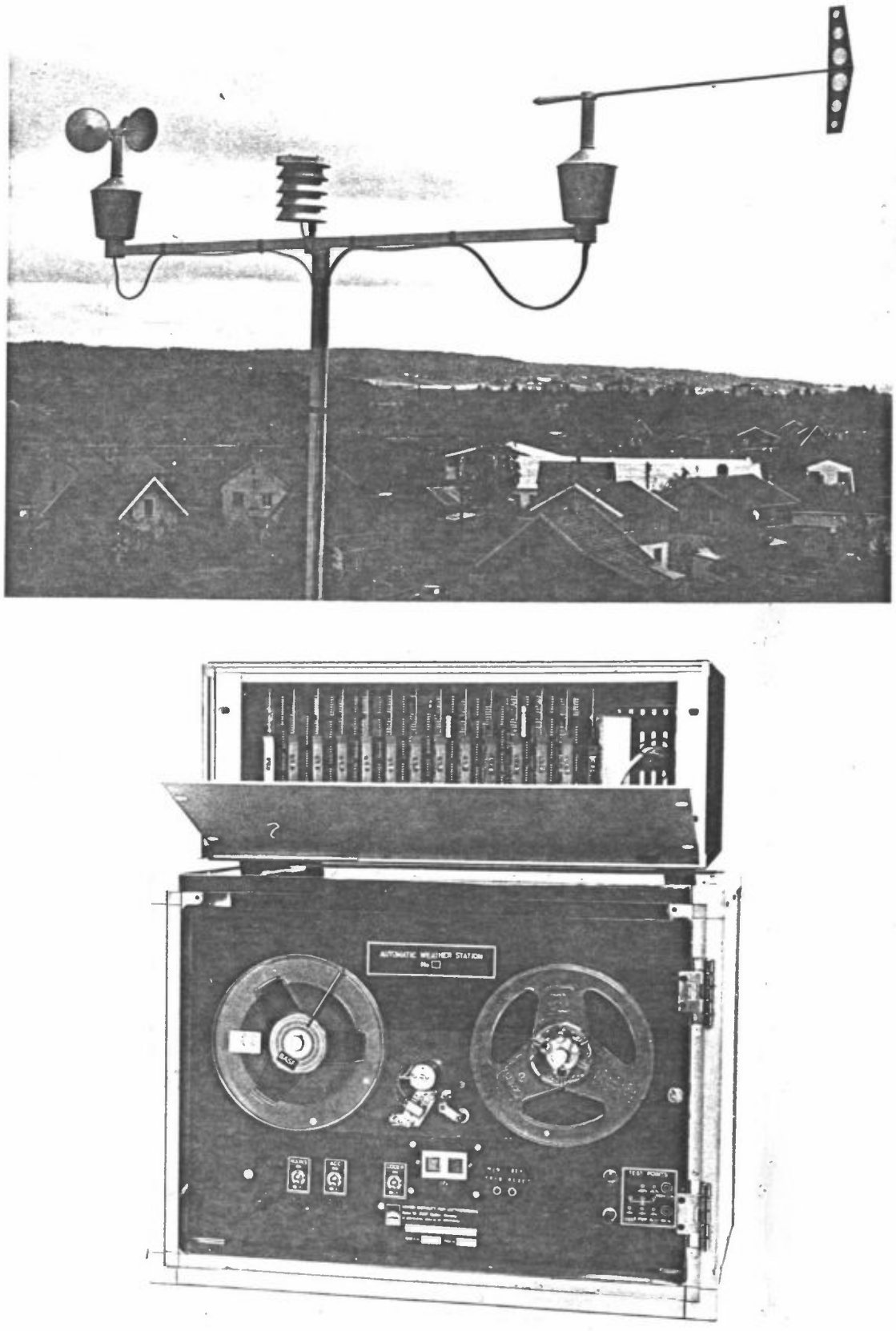

Figure 1: The NILU automatic weather station.

2.2 SF_6 as an Atmospheric Tracer

Sulfur hexafluoride is a colorless, odorless, nontoxic and inert gas which can be detected at extremely low concentrations using electron capture gas chromatography. Pertinent physical data for SF_6 are given in Table 1.

Halasz and Glemsar (9) in a review of SF_6 chemistry, state that "normal nucleophilic reagents cannot attack the highly symmetric octahedral structure of six equal S-F bond distances, 1.56 Å." Case and Nyman (10) suggested that a strong electrophile could coordinate with a fluorine atom and found that the reaction:

$$SF_6 + 2SO_3 \rightarrow 3SO_2F_2$$

proceeded at 20% efficiency at 250°C over 24 hours. At high temperatures, SF_6 also reacts with alkali metals (11). The Matheson Gas Data Book indicates "Sulfur hexafluoride is chemically inert except under conditions of red heat. Even at red heat, sulfur hexafluoride does not attack glass, nor decompose, nor react with hydrogen, ammonia, or oxygen, or any number of other active substances. With hydrogen in a spark, or by heating with hydrogen sulfide, it reacts to form sulfur and will etch a glass container. It does not react with molten potassium hydroxide or with steam at 500°C. Sulfur hexafluoride reacts with molten sodium at about 250°C, with sodium in liquid ammonia at below -60°C, and with sodium diphenylide in 1.2-dimethoxyethane at ambient temperature according to the equation $8Na + SF_6 \rightarrow Na_2S + 6NaF$" (12). However, in the atmosphere, it appears that SF_6 can be considered as an inert, long-lived species. It is one of the least water soluble substances known. The solubity of SF_6 in water and in a series of alcohols has been reported by Lamb and Shair (13).

SF_6 does not occur naturally; it is generally manufactured by burning sulfur in the presence of fluorine. Krey *et al.* (14) reported that the estimated world-wide SF_6 production rate increased from 15 megagrams/year in 1953 to 1180 megagrams/year in 1974.

Table 1: Physical constants of SF_6 (12).

Molecular weight	146.054
Vapor Pressure at 21°C, 1 atm	22.5 kg/cm^2 gauge
Specific Volume at 21°C, 1 atm	156.1 ml/g
Sublimation Temperature at 1 atm	-63.8°C
Freezing Point at 2.21 atm	-50.8°C
Specific Gravity, Gas at 20°C, 1 atm(Air=1)	5.11
Density, Gas at 0°C, 1 atm	6.52 g/l
Density, Liquid at -50.8°C	1.88 g/ml
Critical Temperature	45.55°C
Critical Pressure	37.11 atm (38.35 kg/cm^2 absolute)
Critical Density	0.734 g/ml
Latent Heat of Sublimation at -63.8°C, 1 atm	5640 cal/mole (38.62 cal/g)
Latent Heat of Fusion at -50.8°C, 2.21 atm	1200 cal/mole (8.2 cal/g)
Specific Heat, Liquid at -50.6°C	26.50 cal/(mole)(°C) ((0.18 cal/(g)(°C))
Specific Heat, Gas at 25°C, 1 atm. Cp	23.26 cal/(mole)(°C) ((0.16 cal/(g)(°C))
Viscosity, Liquid at -43.3°C	0.500 centipoise
Viscosity, Gas at 20°C, 1 atm	0.0153 centipoise
Surface Tension at -50°C	11.63 dynes/cm
Thermal Conductivity, Gas at 27°C	0.0433 cal/(sec)(cm^2)(°C/cm)
Heat of Formation, Gas at 25°C	-288.5 kcal/mole (-1972.3 cal/g)
Entropy, Gas at 25°C, 1 atm	69.713 cal/(mole)(°C) ((0.477 cal/(g)(°C))
Dielectric Constant, Gas at 25°C, 1 atm	1.00207
Ionization Potential	19.3 electron volts
Solubility in Water at 25°C, 1 atm	0.001 ml/ml water

Krey et al. (14) measured tropospheric and stratospheric ambient levels and estimated the total atmospheric SF_6 inventory to equal 985 megagrams. Furthermore, Krey et al.(14), considering loss through photolysis the only atmospheric sink, estimated the photolytic half-life to range from 1 to 3 years with a total atmospheric half-life ranging from 12 to 24 years. These authors reported that ratios of SF_6 levels to CCl_3F levels increased markedly with increasing altitudes or polar latitudes indicating that SF_6 is much more stable to photochemical decomposition than CCl_3F. Short-term studies by Saltzman et al.(15) also suggested that SF_6 is stable under ultraviolet radiation.

The principal use of SF_6 is as an electrical insultation medium in switching-gear and transformers. De Bortoli and Peechio (16) reported ambient SF_6 levels over Oslo, Norway to be approximately $4 \cdot 10^{-13}$ p/p. This level is typical of most urban areas.

Sulfur hexafluoride is a nontoxic gas as evidenced by a number of studies using SF_6 to study ventilation rates of the lung (17, 18, 19). Lester and Greenberg (20) exposed animals to an atmosphere consisting of 80% SF_6 and 20% O_2 for periods as long as 24 hours with no indication of irritation or intoxication observed.

The chemistry of SF_6 within the electron capture detector has been reviewed by Lamb (21). This work plus references cited above indicate that SF_6 is an inert, nontoxic gas detectable at extremely low levels and, thus, perfectly suited for use as an atmospheric tracer.

2.3 Tracer release system

In the study described in this report SF_6-tracer was released at a height of 1 m through a gas flow-meter connected to a gas cylinder. The release system is shown in Figure 2.

Figure 2: SF_6 cylinder and gas flow meter.

In each test, SF_6 was released continuously at a steady rate; every release was monitored continuously. The release rate was determined from the scale of the gas flowmeter. This rate was within 10% of the rate determined by weighing the gas bottle before and after each release. A summary of the release data is given in Table 2.

Table 2: SF_6 release data.

Test	Date	Time	Site	Height (m)	Release rate g/s
1	1.3.78	1100-1115	K	1	.0854
2	30.3.78	1000-1045	K	1	.0833
3	12.5.78	1410-1440	K	1	.0833
4	6.6.78	1652-1717	K	1	.0881
5	7.6.78	1430-1455	K	1	.0824
6	29.5.78	1255-1335	V	1	.0728
7	26.7.78	1000-1030	A	40	.191
8	26.7.78	1300-1330	A	40	.191
9	26.7.78	1600-1645	A	40	.191

2.4 Sampling system

Air samples were collected in 20 cm^3 plastic disposable syringes. Detailed, quasi-instantaneous descriptions of the tracer plume were obtained with grab samples collected during walking or automobile crosswind traverses.

Fifteen minute averaged samples were collected at fixed points using either sequential 1-hour samplers (220V, AC), sequential 30 minute samplers (1.5V, DC), or single 15-minute samplers. Small diameter hypodermic needles were used on the syringes to prevent back-diffusion of the sample air. The samplers are shown in Figure 3.

Data from Lamb (21) indicate that samples collected in the syringes do not change in concentration more than 5% over approximately one to two weeks.

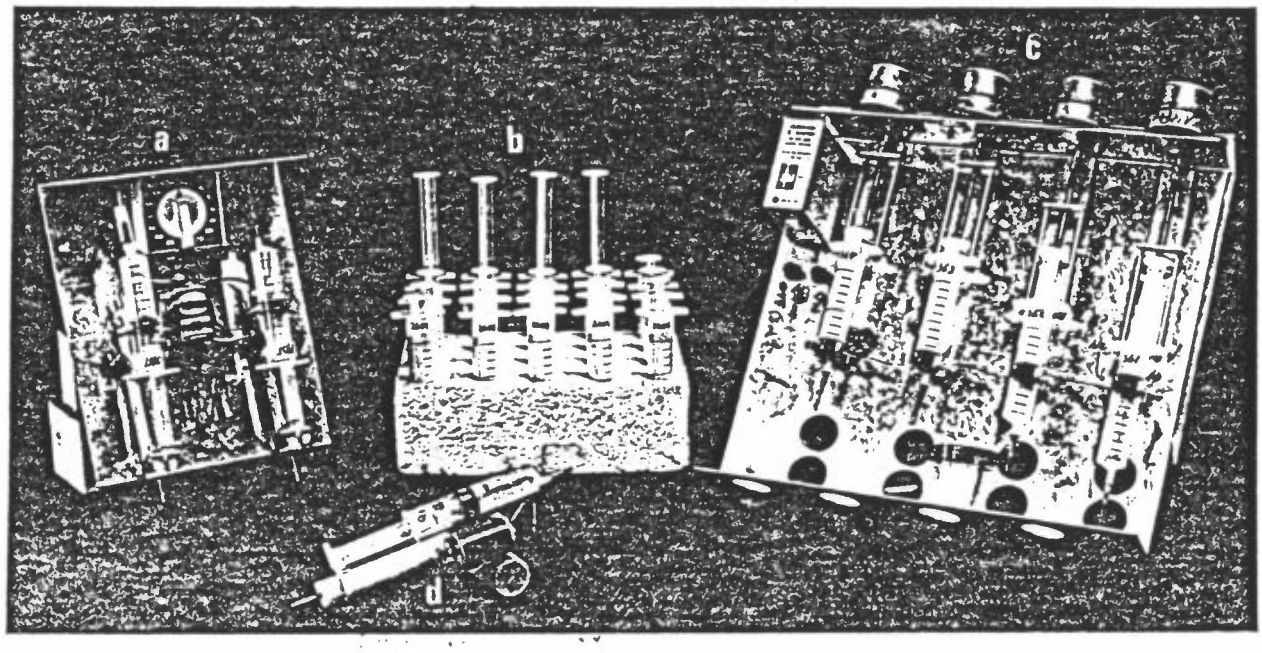

Figure 3: Air sampling equipment

a) 15-minute average sequential sampler, 1.5V, with 60 minute mechanical starting timer.
b) Grab samples.
c) 15-minute average sequential sampler, 220V, with 99 minute electronic starting timer.
d) 15-minute average sampler 1.5V for collecting vertical data via a mast or balloon.

2.5 Analysis of samples

Air samples were analyzed using electron capture gas chromatography. Two gas chromatographs were prepared for each field study. The analysis and calibration system is shown in Figure 4.

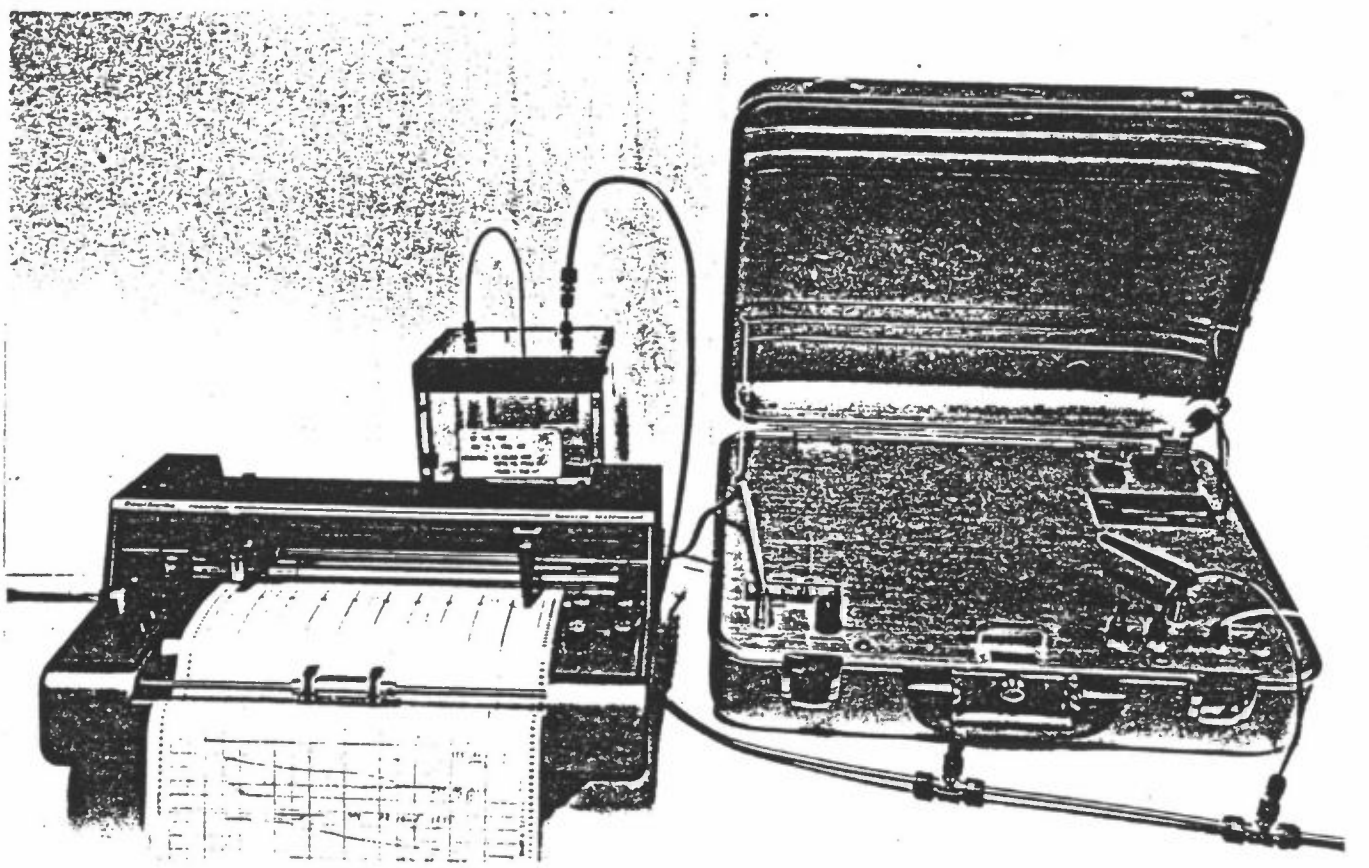

Figure 4: Tracer analysis and calibration system: portable electron capture gas chromatograph, strip-chart recorder, and exponential dilution cube.

A stainless steel coaxial electron capture detector, electrically insulated with teflon and nylon plugs, was pulsed every 200 μsec with a 1 μsec wide pulse. The radioactive source used was a 200 mCi H^3 source bonded to a titanium substrate (U.S. Radium Corp., Bloomsberg, Pennsylvania). Analysis for SF_6 was achieved using a stainless steel column (106 cm x 0.6 cm OD, 0.5 cm ID) packed with 5 A 80-100 mesh Alumina F-1 (Supelco Inc., Crans, Switzerland). Columns were filled with alumina and lightly vibrated before being coiled. The columns were conditioned at 300°C overnight with N_2 flowing continuously. Using prepurified N_2 at 100 cc/min as a carrier gas, O_2 eluted in 4 seconds and SF_6 in 34 seconds. A typical chromatogram is shown in Figure 5.

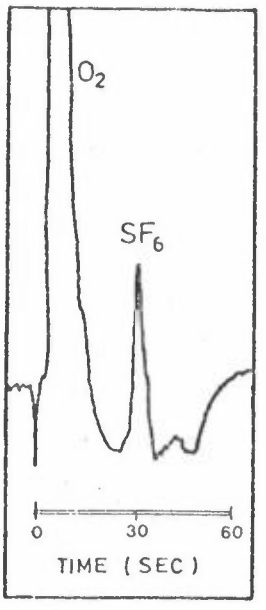

Figure 5: Typical SF_6 chromatogram (SF_6) = 355 ppt.

The gas chromatographs were equipped with 6-port gas sampling valves (Valco, Inc., Houston, Texas) and 1.0 cm^3 sampling loops. The columns and detectors were used at room temperature. With two gas chromatographs, as many as 100 samples could be analyzed by two workers per hour. Concentrations were determined from the peak height output using calibration factors on a strip-chart recorder.

2.6 Calibration of the gas chromatographs

The proportionality constant between peak height and concentration, termed the calibration factor (KF), was determined using an exponential dilution calibration method. For a well-mixed vessel, the concentration, C, decreases according to:

$$C = C_o e^{-qt/V} \qquad (1)$$

where C_o is the initial concentration, q is the constant flow rate, V is the vessel volume, and t is the time since flow began. At any given time, the number of air changes, N, in the chamber since t=0, is qt/V. If the chamber is perfectly mixed and flow is steady, a plot of ℓnC versus N will yield a slope of -1. Using a lucite cube (V=3403 cm^3) equipped with a

magnetically driven fan and flowing clean, dry air through the cube at 120 cm^3/min typically yielded slopes within ±0.01 of the prescribed value. The calibration system is shown in Figure 4. A microliter syringe, accurate to approximately ±1%, was used to inject 3.0 µl of SF_6 into the cube. This method produced calibration samples ranging from approximately 10^{-6} parts SF_6/part air to 10^{-11} parts SF_6/part air (10^6 to 10 parts per trillion, ppt). Samples were drawn from the cube exhaust line directly into the sample valve of each gas chromatograph.

According to a standard error analysis (23), errors associated with the calculated calibration concentrations ranged from less than 3% at high concentrations to less than 7% near the detection limit. Calibrations repeated on consecutive days generally agree within less than ±5%. This calibration system was used by Lamb and Shair (13) to determine the solubility at SF_6 in water. Since their results were within ±6% of results obtained by very accurate volumetric-manometric methods, the absolute accuracy of the calibration appears to be approximately ±6%. A typical calibration curve obtained with the dilution method is shown in Figure 6. This procedure allows calibration of a gas chromatograph over five orders of magnitude of the concentration. The curves become nonlinear at high concentrations because the detector becomes saturated with sample at those levels. In some cases, the curves also become nonlinear near the detection limit. This results from the desorption of tracer from the walls of the cube. Gentle heating of the cube walls and constant purging with clean gas prior to a calibration generally eliminates this problem. Donohoe (24) reported that the degree of absorption and desorption of a number of Freons was decreased considerably in a cube lined with Tedlar.

A potentially serious problem associated with prolonged use of the gas chromatographs is contamination of the radioactive foil by deposition of eluted contaminates. As the foil becomes contaminated, the detector operating characteristics change.

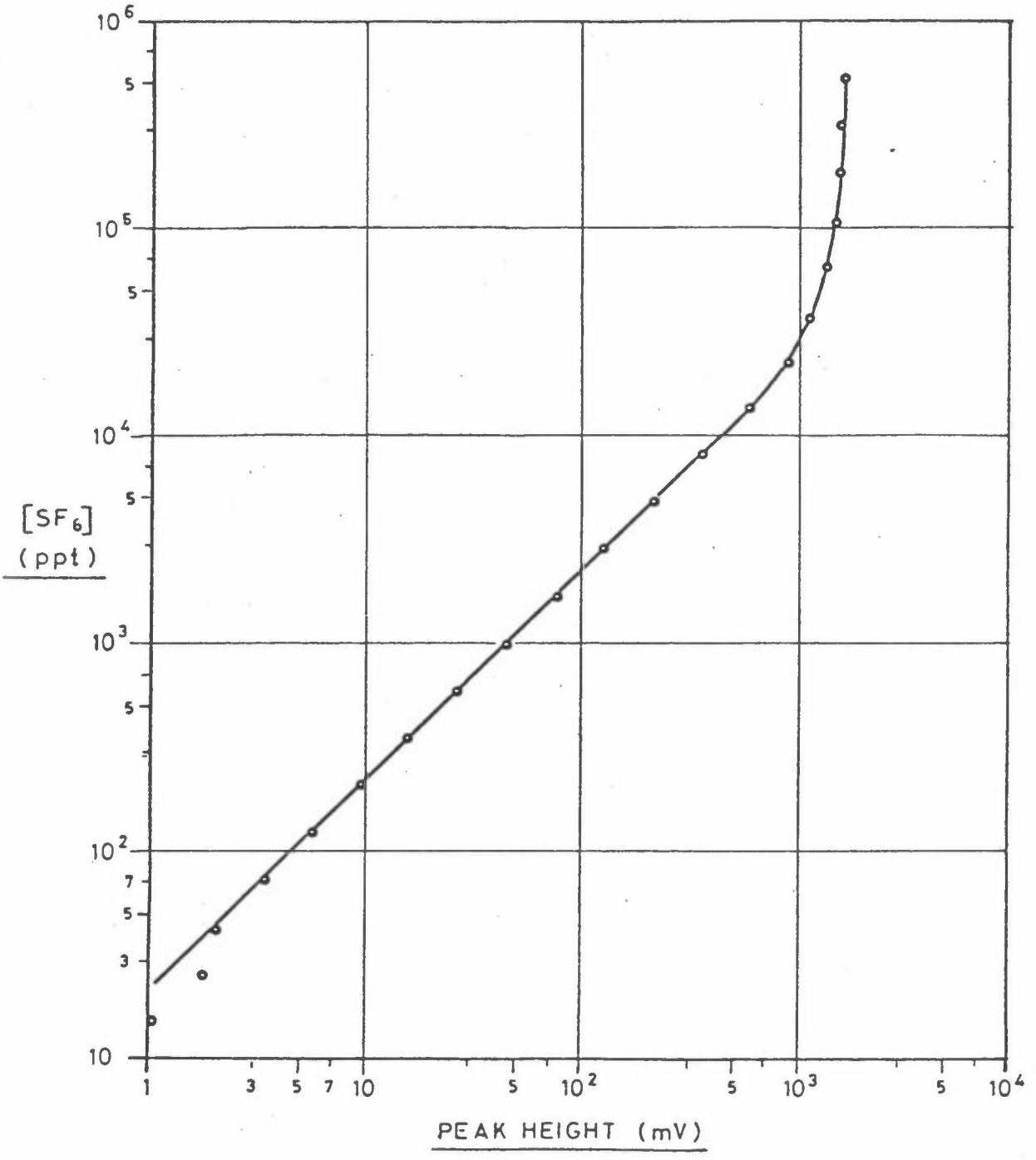

Figure 6: Typical SF_6 calibration curve.

The concentrations of samples analyzed under these conditions can be in error as much as 15% to 25%. One means of monitoring changes in the detector response is to cross-check samples between the gas chromatographs. Calibration cross-check data for these tests indicate that concentrations are accurate to within 15%.

3 CALCULATION OF PLUME PARAMETERS FROM TRACER DATA

3.1 Calculation of σ_y

Plumes are often modeled by assuming they have a gaussian shape; that is, the concentration along a crosswind traverse follows an equation:

$$C(y) = C_o \exp\left[-\tfrac{1}{2}\left(\frac{y-Y_o}{\sigma}\right)^2\right] \qquad (2)$$

where Y_o is the distance coordinate of the center of the plume, C_o is the concentration at the center of the plume, and σ is the standard deviation of the measured plume concentrations. From standard data analysis techniques, equations relating σ and Y_o to the data obtained (C(y) and y) are:

$$Y_o = \frac{\int_{-\infty}^{\infty} yC(y)dy}{\int_{-\infty}^{\infty} C(y)dy} \qquad (3)$$

and

$$\sigma = \left[\frac{\int_{-\infty}^{\infty} y^2C(y)dy}{\int_{-\infty}^{\infty} C(y)dy} - Y_o^2\right]^{\frac{1}{2}}. \qquad (4)$$

A value for C_o can also be calculated, once Y_o and σ have been calculated:

$$\int_{-\infty}^{\infty} C(y)dy = C_o\,\sigma\sqrt{2\pi} \qquad (5)$$

or, rearranging terms,

$$C_o = \frac{\int_{-\infty}^{\infty} C(y)dy}{\sqrt{2\pi}\,\sigma} \qquad (6)$$

These parameters (C_o, Y_o, σ) when used in Equation (2) represent a best-fit of the data (C(y),y) to the equation. Typical results of the analysis are shown in Figure 7.

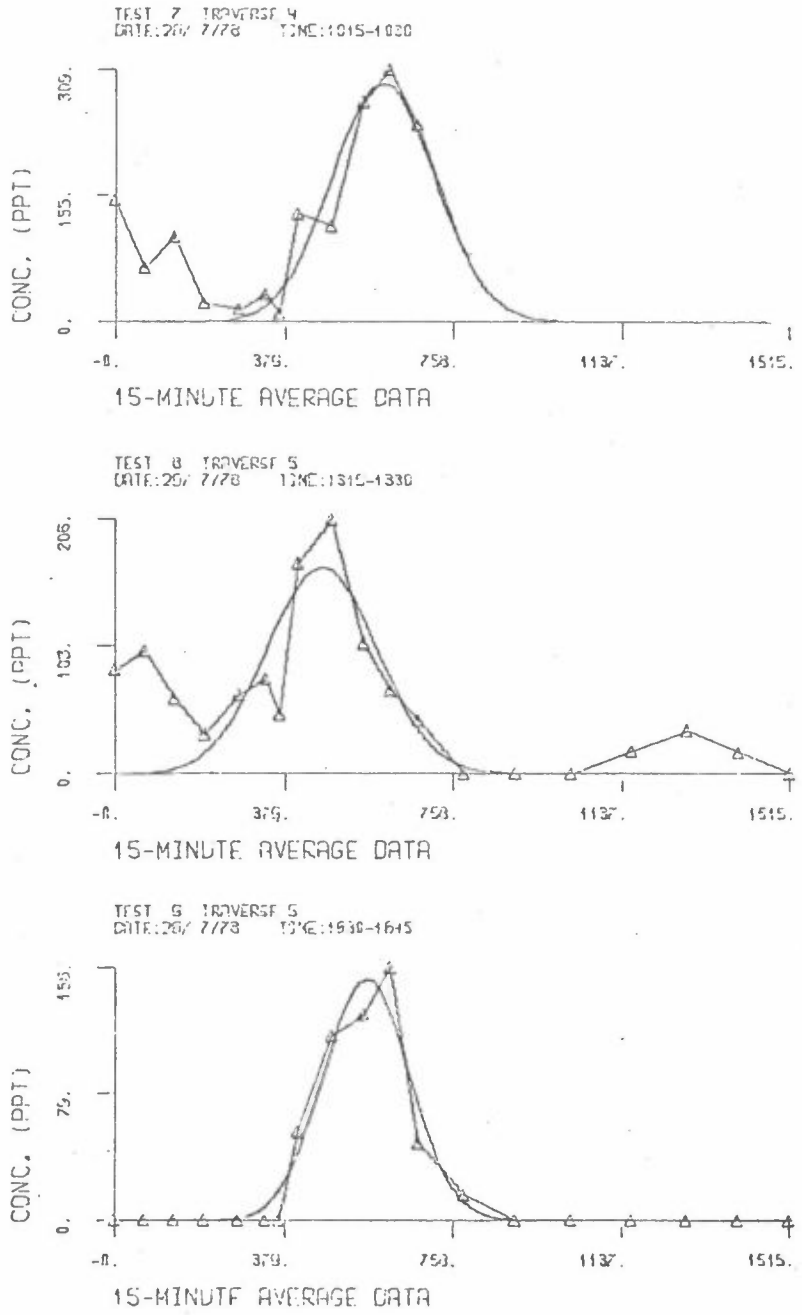

Figure 7: Cross-wind SF_6 concentration profiles and best-fit Gaussion curves.

Measured values of σ (σ_m) were corrected for the angle of the traverse path with respect to the wind direction as follows:

$$\sigma = \sigma_m \sin \alpha \qquad (7)$$

where α is the specified angle.
Errors involved in the application of these equations are discussed in Appendix B.

3.2 Calculation of σ_z

If one assumes that the Gaussian plume model can be used to describe the tracer results, and that tracer is conserved during transport, then a value of σ_z can be calculated in an iterative manner using the crosswind integral of horizontal crosswind traverse data:

$$\underset{CWI}{C} \equiv \int_{-\infty}^{\infty} C(y)dy = \frac{Q}{\sqrt{2\pi}\,\sigma_z u} \left\{ \exp\left[-\tfrac{1}{2}\left(\frac{z+H}{\sigma_z}\right)^2\right] + \exp\left[-\tfrac{1}{2}\left(\frac{z-H}{\sigma_z}\right)^2\right] \right\} \qquad (8)$$

Since the crosswind integral of the crosswind data is calculated in the procedure to find σ_y, it is relatively simple to also calculate σ_z.

In several cases vertical concentration profile data were obtained from samplers attached to a 10 m mast downwind of the release. A value of σ_z can be calculated from these data by performing a least-squares best-fit of these data with the following expression:

$$C(z) = C_o \left(\exp\left[-\tfrac{1}{2}\left(\frac{z+H}{\sigma_z}\right)^2\right] + \exp\left[-\tfrac{1}{2}\left(\frac{z-H}{\sigma_z}\right)^2\right] \right) \qquad (9)$$

where C_o and σ_z are the parameters adjusted to fit the data.

Calculations of σ_y and σ_z along with tabulation and plotting of the data and best-fit curves are accomplished by means of the NILU computer program PLMFIT.

4 PRESENTATION OF DATA

4.1 σ_θ statistics

The cumulative frequency distribution of 5-minute average values of σ_θ at different sites is presented in Figure 8.

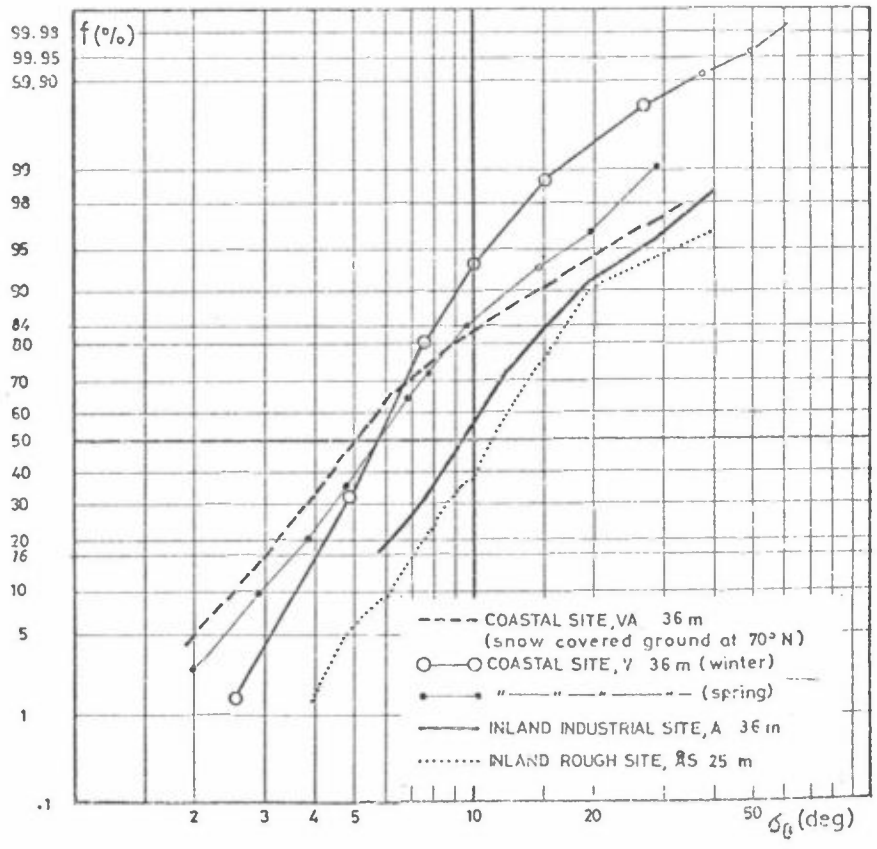

Figure 8: Cumulative frequency distribution of σ_θ at different sites.

The σ_θ-statistics vary from one site to another. Apart from being a function of sampling height above the ground, as

demonstrated by Pendergast and Crawford (25), the frequency distribution of σ_θ is also dependent upon the surface roughness at the site. The median value of σ_θ varies 5 deg. for a smooth snow covered surface, to 12 deg. for a rough inland site. Measurements of σ_θ in the atmospheric surface layer may only represent the local turbulence generated by the roughness of the upwind surfaces. These characteristics of σ_θ should be considered when σ_θ data are to be applied in dispersion calculations.

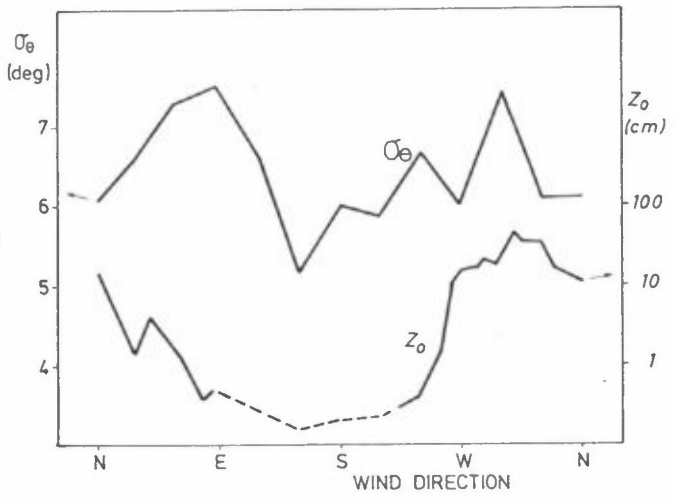

Figure 9: Average σ_θ and surface roughness, Z_o, values as a function of wind direction. (site V).

In figure 8 the average σ_θ values from one site are presented together with calculated surface roughness length as a function of wind direction. The roughness lengths (z_o) were estimated from wind profile measurements during near neutral conditions assuming a logaritmic wind profile:

$$u_z = u_* \cdot \ln(z/z_o)/\kappa \qquad (10)$$

where u_* is the friction velocity and κ is von Karman's constand, z_o was taken from measurements of wind speed u_1 and u_2 at two levels z_1 and z_2:

$$z_o = \exp\left(\frac{u_2 \ln z_1 - u_1 \ln z_2}{u_2 - u_1} \right) \qquad (11)$$

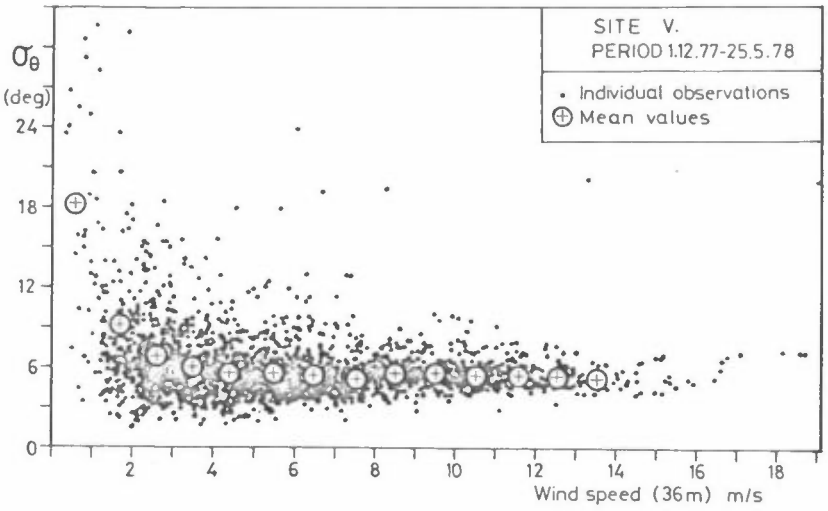

Figure 10: σ_θ versus wind speed measured at a 36 m tower, coastal site.

Observations of σ_θ and wind speed at the 36 m level from a coastal site are presented in Figure 9. An inverse relation between σ_θ and wind speed is evident, showing an enhanced wind direction variation for wind speeds less than ≈ 3 m/s. For wind speeds higher than 3 m/s, σ_θ approaches 6 deg. To further demonstrate the diversity in σ_θ, values are presented as functions of wind direction and wind speed in Figure 11.

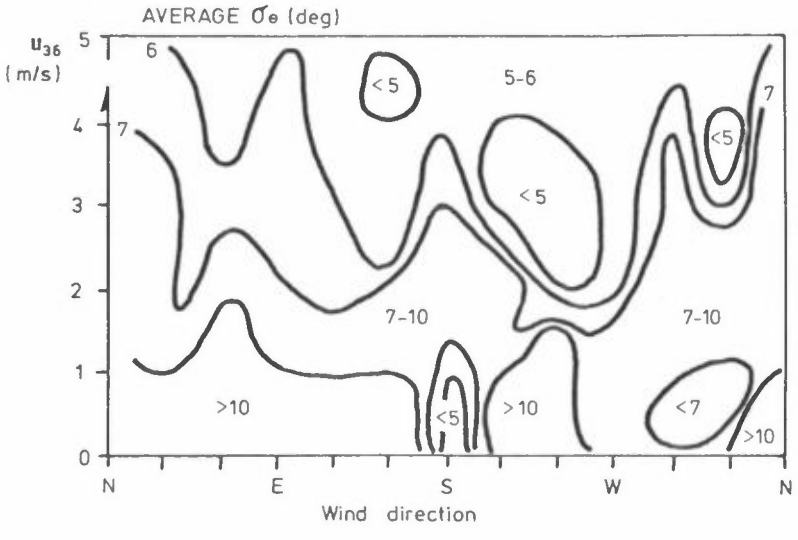

Figure 11: Average σ_θ values (in deg) as functions of wind direction and wind speeds at site V.

For low wind speeds, average σ_θ values varies considerably; from >10 deg for winds from N, E and SW to <5 deg for winds from S.

For wind speeds above 4 m/s, the average σ_θ is between 5 and 6 deg, except for wind from N, where the up-wind surface roughness is large.

4.2 σ_θ versus stability classification parameters

The stability classification from temperature lapse rate measurements, as a method for determining dispersion parameters from PGT-curves, has been demonstrated to greatly underpredict σ_y under very light wind speed, stable conditions. (6).

The relationship between σ_θ and a bulk Richardson number, $RB = dT_{36-10}/u^2$, and between σ_θ and dT_{36-10} is presented in Figure 12.

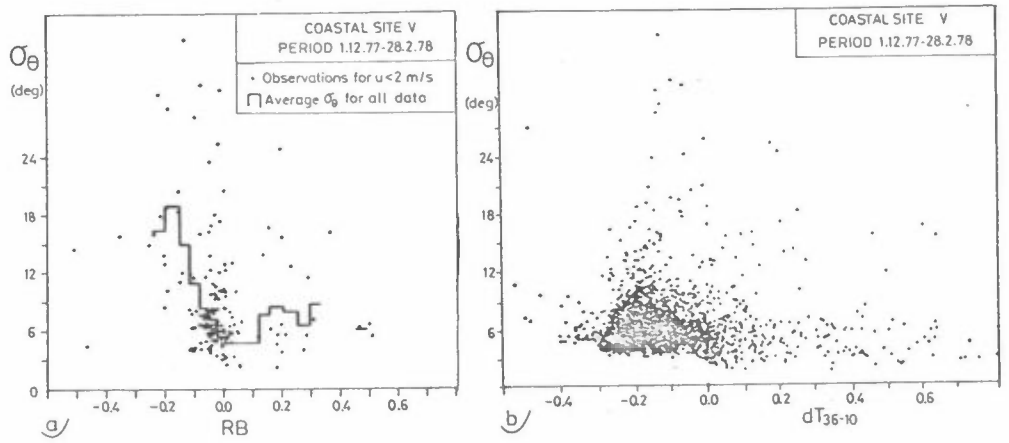

Figure 12: Obervations of σ_θ versus:
a) Bulk Richardson number $RB=dT_{36-10}/u^2$
b) Temperaturedifference dT_{36-10} between two levels; 36 m and 10 m.

These data show the inadequacy of dT or RB to represent σ_θ. The spread of data points is considerable. In Figure 12a the largest average σ_θ value: 18 deg, occurs for RB ≃ -0.2. Values of σ_θ decrease to 5.6 deg for RB = 0 (neutral stability) and then increase again for positive values of RB (stable conditions).

The individual observations plotted as points in Figure 11, show that high values of σ_θ, i.e. large horizontal spread, might occur for all values of RB and dT. This emphasizes the importance of applying a "split sigma" method for estimating the dispersion of air pollutants. When applying the data from meteorological towers, horizontal and vertical dispersion should be estimated separately.

4.3 Dispersion data from SF_6 tracer experiments

To test different methods for estimating σ_y and σ_z, based upon data from the NILU automatic weather station, diffusion experiments were carried out at 3 different sites. Table 4 summarizes the data obtained during these studies. The data and maps of each site are given in Appendix A.

Table 3: Dispersion experimental data. Met. data taken at 10 and 2 m.

Test no	Date	Hour	Site	$\bar{u}$ (m/s)	dT_{10-2} deg	σ_θ rad	Height for σ_θ-meas.(m)	distance,x (m)	σ_y(obs) (m)	σ_z(estim) (m)
1	1.3.78	11	K	2.2	-0.15	0.23	10	130	15	3
								850	110	25
2	30.3.78	10	K	4.1	-0.5	0.26	10	130	14	26
								850	93	108
4	6.6.78	17	K	4.0	-0.7	0.27	10	130	37	8
								850	155	57
		18	K	4.0	-0.5	0.34	10	850	187	48
5	7.5.78	14	K	3.7	-0.9	0.29	10	130	35	13
								850	108	34
		15	K	3.2	-1.4	0.4	10	850	151	13
6	29.5.78	13	V	4.2	-0.7	0.18*	36	100	29	4
								300	65	9
		14	V	3.7	-0.8	0.21*	36	100	34	4
							36	300	64	9
7	26.7.78	10	A	1.6	-0.7	0.26*	36	950	116	28
		13	A	2.0	-0.6	0.15*	36	950	124	23
		17	A	1.8	-0.7	0.16*	36	900	97	21

*) σ_θ measured at 36 m

The crosswind standard deviations σ_y were obtained from 15-minute average SF_6 concentrations taken along cross wind traverses. The values were calculated from the best fit gaussian curve to the concentration data. The vertical standard deviations σ_z were estimated from mass balance calculations as shown in ch. 3.2.

It should be noted that σ_θ data from site A and V were measured at 36 m. This might lead to reduced σ_θ values compared to the measured σ_y from ground level releases.

For comparison the observed values of σ_y and σ_z are presented on PGT curves in Figure 13.

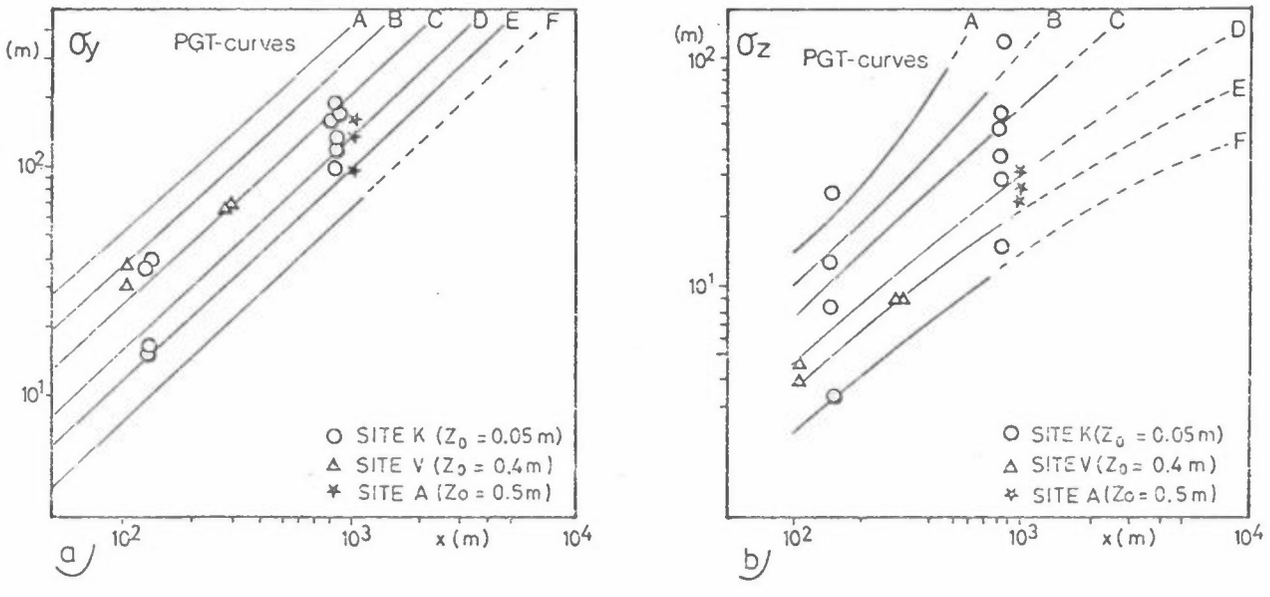

Figure 13: a) Crosswind standard deviation σ_y of tracer material, and b) vertical standard deviation σ_z of tracer material, plotted on standard PGT curves as a function of down wind distance.

5 ESTIMATES OF σ_y FROM METEOROLOGICAL DATA

Several methods for estimating σ_y from measurements of the horizontal wind direction fluctuations σ_θ (in radians) have

been suggested. For example Cramer et al (26) used a power law in x:

$$\sigma_y = \sigma_\theta \cdot x_r \quad (x/x_r)^P \qquad (12)$$

where x_r is a reference length and x is the distance in metres.

Pasquill (29) following Taylor's statistical treatment of diffusion, recommended:

$$\sigma_y = \sigma_\theta \cdot x \cdot f(t/t_L) \qquad (13)$$

where t is the travel time ($\simeq x/\bar{u}$) and t_L is the Langrangian integral time scale. Draxler (30) analyzed experimental data, and found that the function f could be expressed by

$$f = \frac{1}{1+a(t/T_i)^{\frac{1}{2}}} \qquad (14)$$

where T_i is the diffusion time required for f to become 0.5, and a is a empirical constant.

From the experimental data presented in Table 3, the σ_y/σ_θ ratio is plotted in Figure 14 as a function of distance.

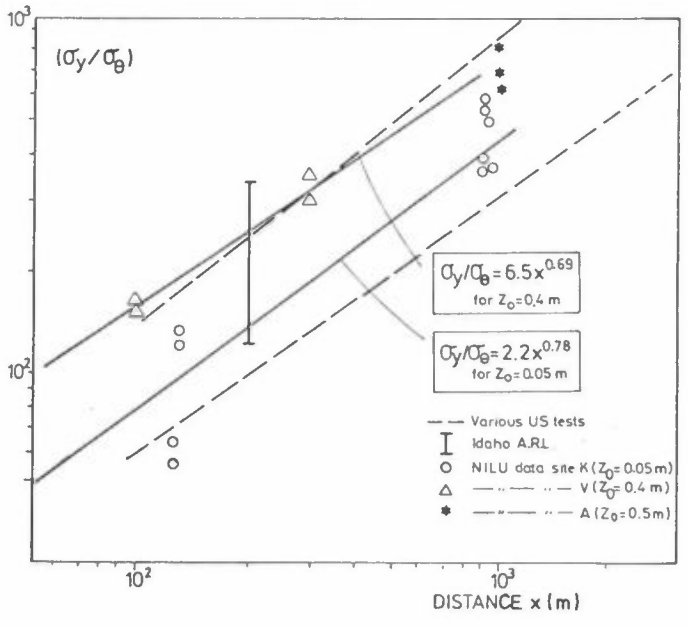

Figure 14: The ratio σ_y/σ_θ as a function of distance x (m).

The range of data from various U.S. tests (27,28) is also indicated in Figure 14. The best fit curves to our diffusion data for site K ($z_o \simeq 5$ cm) yield:

$$\sigma_y = 2.2 \cdot \sigma_\theta \cdot x^{0.78} \qquad (15)$$

At site V and A, where the estimated roughness length is 0.4 m and 0.5 m, respectively, σ_y can be expressed by:

$$\sigma_y = 6.5 \cdot \sigma_\theta \cdot x^{0.69} \qquad (16)$$

The slope of this x-dependancy is in agreement to McElroy's data from St. Louis for urban dispersion (34).

The function f given in Eq. *(13)* is estimated from the diffusion data in Table 3, and presented as a function of the travel time t in Figure 15.

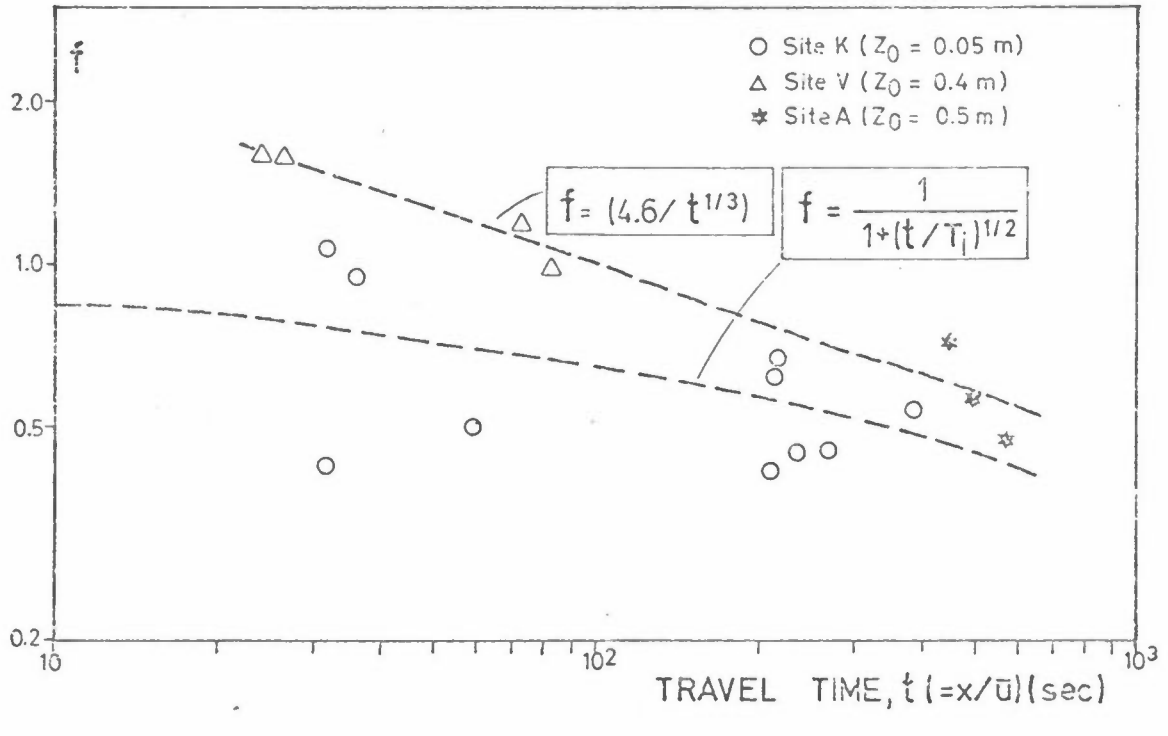

Figure 15: f as a function of travel time t for tracer releases within the atmospheric surface layer.

At site K, which is fairly smooth (roughness length ≃ 5 cm), $\alpha = 1$, and $T_i = 330$ s. The data agree with:

$$f = \frac{1}{1 + 0.055 \cdot t^{\frac{1}{2}}} \qquad (17)$$

For the rougher sites V and A the function f can be approximated by

$$f = 4.6/t^{1/3} \qquad (18)$$

For travel times less than 97 the function f at these rough sites is greater than 1. This does not agree with Taylor's theoretical treatment of diffusion, which states that f should approach 1 for short travel times. One reason for the discrepancy might be that σ_θ was measured at a level too high above the ground (36 m) compared to diffusion of SF_6 that took place within the 0-25 m surface layer.

Based upon comparisons with several observations, Paquill (4) has suggested values for f as a function of travel distance x. His values are given in Table 4 together with extrapolated values from our data.

Table 4: The function f for different travel distances as given by Pasquill (4), and from NILU data.

x (km)	0.1	0.2	0.4	1	2
f(x)Pasquill	0.8	0.7	0.65	0.6	0.5
site K(z_o=5 cm)	0.78	0.68	0.63	0.52	
site V(z_o=40 cm)	1.6	1.25	1.0		
site A(z_o=50 cm)				0.65	

In Figure 16 the estimated values of σ_y are plotted versus values determined from SF_6-concentrations.

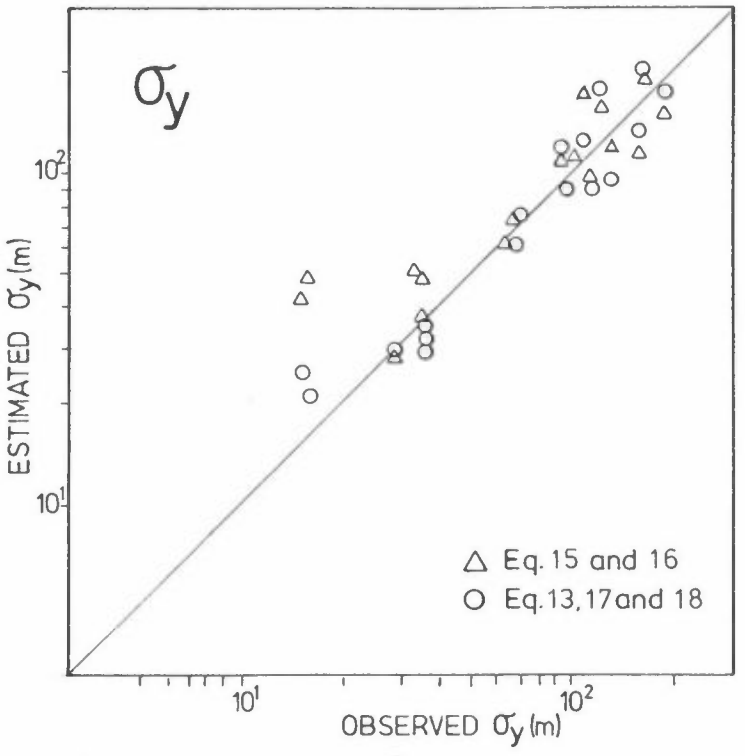

Figure 16: Estimated versus observed (from SF_6-concentrations) values of σ_y.

As shown in the Figure, equation *(13)*: $\sigma_y = \sigma_\theta \cdot f(t/t_2) \cdot x$ appears to fit the measured σ_y data best. At least for near neutral conditions, values of σ_y can be estimated from measurements of wind direction fluctuations, σ_θ. The function f seems to be surface roughness dependent as indicated from Eq. *(17)* and *(18)*. This aspect will, however, be further studied in future investigations.

6 ESTIMATES OF σ_z FROM METEOROLOGICAL DATA

The vertical dispersion of air pollutants is described by the diffusion equation:

$$\frac{dC}{dt} = \frac{\partial}{\partial z} \left(K_z \frac{\partial C}{\partial z}\right) \qquad (19)$$

where C is the concentration of material, K_z the eddy diffusivity and z is the vertical coordinate. For a simple diffusion process in a stationary situation with homogeneous wind and turbulence, the solution of Eq.(19) is of Gaussian form, with variance:

$$\sigma_z^2 = 2K_z t \quad \text{where } t=x/\bar{u} \qquad (20)$$

In the surface layer, the vertical eddy diffusivity K_z is strongly related to the eddy conductivity K_h:

$$K_z \simeq K_h = \kappa \cdot u_* \cdot z/\phi_h(z/L) \qquad (21)$$

where κ is von Karman's constant, u_* is the friction velocity, L is the Monin-Obukhov length, and ϕ_h is a universal function of z/L. A model for the surface layer, as proposed by Busch et al. (31) and based upon established similarity theory, was applied to estimate friction velocites, surface heat fluxes H_o, and Monin-Obhukov lengths from measurements of wind and temperature profiles.

An iterative process was applied to estimate L from:

$$L = - c_p \rho T_o u_*^3/(\kappa \cdot g \cdot H_0) \qquad (22)$$

with $H_0 = -\rho c_p u_* \Theta_*$ (23)

where the wind and temperature profiles are given by:

$$u = \left[\ln(z/z_0) - \psi_m(z/L)\right] \cdot u_*/\kappa \qquad (24)$$

$$\Delta\theta = 0.74 \left[\ln(z/z_0) - \psi_h(z/L)\right] \cdot \theta_* \qquad (25)$$

The functions Ψ_m and Ψ_h are the integrals of the universal functions ϕ_m and ϕ_h given by Businger (32):

$$\text{for } (z/L) < 0 : \quad \phi_m = (1-15\ z/L)^{-1/4} \qquad (26)$$

$$\phi_h = 0.74(1-9\ z/L)^{-1/2} \qquad (27)$$

$$\text{for } (z/L) > 0 : \quad \phi_m = 1 + 4.7\ z/L \qquad (28)$$

$$\phi_h = 0.74 + 4.7\ z/L \qquad (29)$$

Two approaches have been investigated for estimating K_z from Eq. *(21)*. In the first case K_z is estimated at a fixed reference height, z_{ref}, equal to the anemometer height:

$$K_z = \kappa\ u\ z_{ref}/\phi_h(z_{ref}/L) \qquad (30)$$

This formula was applied for all stabilities (all values of L). In the second approach, the plume height increase with downwind distance from the source has been taken into account. The height z at which K_z should be estimated in Eq. *(21)* was assumed to vary with distance. In this case K_z was assumed to increase linearly with height in the surface layer of the atmosphere. The effective height, z_e, at which K_z is estimated to simulate the vertical spread of the plume, was assumed to be $0.5\ \sigma_z$.

For unstable conditions (L<0) the function $\phi_h(z/L)$ varies little from the initial value:

$$\phi_h(z/L) \simeq \phi_h\ (z_{ref}/L) \simeq \text{const.} \qquad (31)$$

The expression for K_z from *(21)* inserted in *(20)*, with $z = 0.5\ \sigma_z$, gives:

$$\sigma_z = \frac{\kappa}{\phi_h} \frac{u_*}{\bar{u}} \cdot x \qquad (32)$$

where $\bar{u}$ is the average effective transport velocity.

Equation *(30)* states that σ_z increases linearly with travel distance x for unstable stratification. Deardorff and Willis (33) found from laboratory experiments that σ_z increased as $x^{3/2}$. In an unstable surface layer with an upper inversion at z_i they proposed for $\sigma_z < 0.5\ z_i$:

$$\sigma_z = 0.4 \left[\left(1 - \frac{13}{L} \left(\frac{u_*}{\bar{u}}\right) x\right]^{\frac{1}{2}} \left(\frac{u_*}{\bar{u}}\right) \cdot x \right. \qquad (33)$$

For stable concitions (L>0) the function ϕ_h (z/L) given in Eq. *(22)* inserted in Eqs. *(21)* and *(20)* gives:

$$\sigma_z = 0.2\ L \left[\left(1 + \frac{9.4K}{L} \left(\frac{u_*}{\bar{u}} \right) x\right)^{\frac{1}{2}} - 1 \right] \qquad (34)$$

If estimated values of σ_z from the above theory are plotted versus values of σ_z estimated from SF_6-experiments, as shown in Figure 17, the results show a much larger scatter than was the case for σ_y in Figure 16.

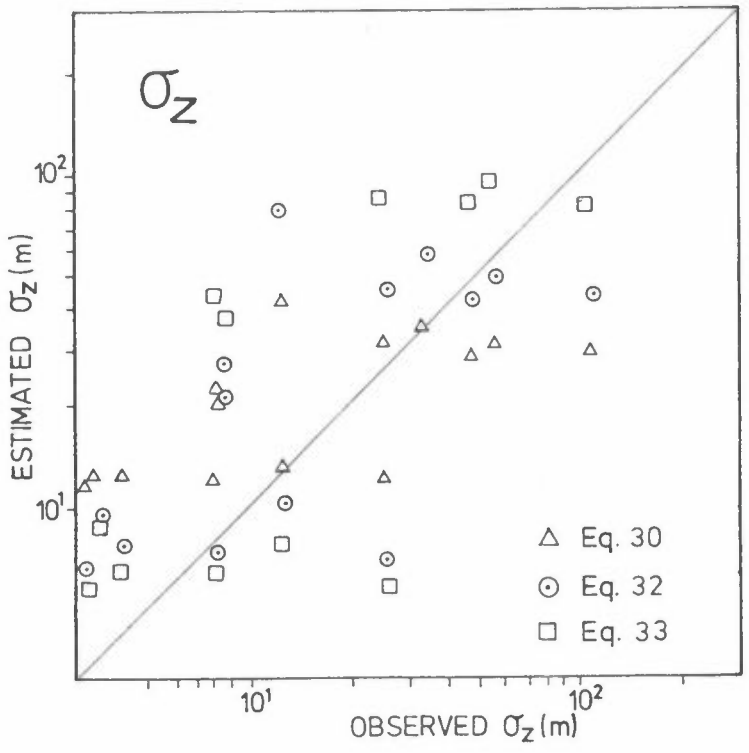

Figure 17: Estimated values of σ_z (from wind and temperature profile data) versus "observed" values (from SF_6-experiments).

The best fit is given by Eq. *(32)*, where σ_z is linearly related to the distance. Better measurements of vertical concentration profiles are, however, needed to draw any final conclusions as to the σ_z-estimates.

7 CONCLUSIONS

The main purpose of this study was to investigate the applicability of the NILU automatic weather station's wind statistics and temperature profiles in dispersion estimates.
It is demonstrated from tracer experiments that the measurements of the standard deviation in the horizontal wind fluctuations can be used to estimate the horizontal dispersion parameter, σ_y. This is already being applied in routine dispersion estimates at NILU. Measurements of vertical wind- and temperature profiles might be used to estimate values of the vertical dispersion parameter, σ_z. Here more work is, however, needed.
Future SF_6-tracer investigations will be conducted to study: different stability conditions, (included L>0), effect of different release heights, roughness dependency and the spread at larger distances.

8 REFERENCES

(1) Turner, D.B. — Workbook of atmospheric dispersion estimates. Washington, D.C., Dept. Health, Ed. & Welfare, 1969. (Environ. Health Service, Pub. No. 995-AP-26.)

(2) Gifford, F.A. — Use of routine meteorological observations for estimating atmospheric dispersion. *Nucl. Safety*, 2, 47-51 (1961).

(3) — Nuclear Regulatory Commision, Safety Guide 1.23, Onsite meteorological programs, (1972).

(4) Pasquill, F. — Dispersion parameters in gaussian plume modeling, part 2, possible requirements for change in the Turner workbook values. Washington D.C. 1976. (EPA-600/4-76-030b.)

(5) Hanna, S.R. et al. — AMS Workshop on stability schemes and sigma curves - Summary of recommendations. *Bull. Am. Met. Soc.* 58, 1305-1308 (1977).

(6) Van der Hoven, I. — A survey of field measurements of atmospheric diffusion under low-wind-speed inversion conditions. *Nucl. Safety*, 17, 223-230 (1976).

(7) Hanna, S.R. — A review of the influence of new boundary layer results on diffusion prediction techniques. In: *Proceedings of WMO Symposium on boundary layer physic applied to specific problems of air poll.* Norrköping 1978. (WMO-No 510.)

(8) Berg, T.C., Sivertsen, B. — An electronic monitor for measuring atmospheric turbulence. In: *Proceedings of WMO Technical Conference on Instruments and Methods of Observation (TECIMO).* Hamburg 1977. (WMO-No. 480.)

(9) Halasz, S.P.
Glemsar, O.
Sulfur in organic and inorganic chemistry vol. 1, A. Senning, ed.. New York, Marcel Dekker, Inc., 1971, p. 217.

(10) Case, J.R.
Nyman, F.
Some chemical reactions of sulphur hexafluoride.
Nature 193, 473, (1962).

(11) Roberts, H.L.
Inorganic sulfur chemistry, G. Nickless, ed.. Amsterdam, Elsevier Publishing Company, 1968, p. 420.

(12) Matheson Company, Inc.
Matheson Gas Data Book.

(13) Lamb, B.K.
Shair, F.H.
Determination of concentrations of halogenated compounds dissolved in various liquids by electron capture gas chromatorgaphy.
Anal. Chem. 48, 473-475 (1976).

(14) Krey, P.W.
Lagomarsino, R.J.
Toonkel, L.E.
Schonberg, M.
Atmospheric residence of SF_6.
In: *Health and Safety Laboratory Environmental Quarterly*, E.P. Hardy, ed.. New York, ERDA, 1976. pp. 50-57.

(15) Saltzman, B.E.
Coleman, A.I.
Clemons, C.A.
Halogenated compounds as gaseous meteorological tracers: Stability and ultrasensitive analysis by gas chromatography.
Anal. Chem. 38, 753-758 (1966).

(16) De Bortoli, M.
Peechio, E.
Measurements of some halogenated compounds in air over Europe.
Atmos. Environ. 10, 921-923 (1976).

(17) Wood, L.D.H.
Ruff, F.
Bryan, A.C.
Milie-Emili, J.
Influence of air density on the distribution of ventilation.
Physiologist, 12, 398 (1969).

(18) Martin, R.R.
Zutter, M.
Anthonisen, N.R.
Pulmonary gas exchange in dogs breathing SF_6 at 4 Atm.
J. Appl. Physiol. 33, 86-92 (1972).

(19) Paciorek, M.
Masters Thesis. California Institute of Technology, Pasadena, California 91125, 1977.

(20) Lester, D.
Greenberg, L.A.
The toxicity of sulfur hexafluoride. *Arch. Industr. Hyg. Occup. Med.* 2, 348-349 (1950).

(21) Lamb, B.K.
Development and application of dual atmospheric tracer techniques for the characterization of pollutant transport and dispersion. California Institute of Technology, Ph. D. Thesis. Pasadena, California 1978.

(22) Drivas, P.J.
Investigation of atmospheric dispersion problems by means of a tracer technique. California Institute of Technology Ph.D. Thesis. Pasadena, California 1974.

(23) Bevington, P.R.
Data reduction and error analysis for the physical sciences. New York, McGraw-Hill, 1969, pp. 56-65.

(24) Donohoe, K.G.
Personal communication. Moffett Field, California, NASA Ames Research Lab. 1975.

(25) Pendergast, M.M.
Crawford, T.V.
Actual standard deviations of vertical and horizontal wind direction compared to estimates from other measurements. Preprints of Symposium on Atmospheric Diffusion and Air Pollution, St. Barbara, California, 1974.

(26) Cramer, H.E.
De Santo, G.M.
Dumbauld, K.R.
Morgenstern, P.
Swanson, R.N.
Meteorological prediction techniques and data system, GCA techn. rep. no 64-3-G, Bedford, Mass., 1964.

(27) Sagendorf, J.F.
Dickson, C.R.
Diffusion under low windspeed. Inversion conditions, NOAA Technical Momorandum ERL, ARL-52, (1974).

(28) Slade, D.H. (Ed)
Meteorology and atomic energy. U.S. Atomic Energy Commission, 1968. Springfield, Virg. (TID-24190).

(29) Pasquill, F.
Some topics relating to modelling of dispersion in boundary layer. Research Triangle Park, N.C., 1975. (EPA-650/4-75-015.)

(30) Draxler, P.R.
Determination of atmospheric diffusion parameters. *Atmos. Environ.* 10, 99-105 (1976).

(31) Busch, N.E.
Chang, S.W.
Anthes, R.A.
A multi-level model of the planetary boundary layer suitable for use with mesoscale dynamic models. *J. Appl. Met.* 15, 909-918 (1976).

(32) Businger, J.A.
Turbulent transfer in the atmospheric surface layer. In: *Workshop on micrometeorology*, D.A. Haugen, Ed.. Boston, Am. Met. Soc, 1973, pp. 67-98.

(33) Deardorff, J.W.
Willis, G.E.
Computer and laboratory modeling of the vertical diffusion on non-buoyant particles in the mixed layer. In: *Symp. on Turb. Diff. in Environmental Poll. Proc.* Charlottesville Va., 1973. (Adv. in Geophysics. 18B), pp. 197-200.

(34) McElroy, J.L.
A comparative study of urban and rural dispersion. *J. Appl. Met.* 8, 19-31 (1969).

APPENDIX A

SYNOPSIS OF TRACER TESTS

A.1 Site K

A map of site K is given in Figure A1. The test area is a flat, grassy, open area bounded on the west by a residential area and on the east by a major road and residential area lying amid gently rolling hills. The surface roughness is estimated to be about 5 cm. The main sampling lines were along line A-B, 130 m from the release point R1, and line C-D, 950 m from release point R1. Data obtained from tests conducted at site K are tabulated in Table A-1.

A.1.1 Test 1, 1 March 1978

SF_6 was released from point R1 from 1100 to 1115 at a rate of .0854 g/s. The release height was 1 m. Instantaneous air samples were collected during walking traverses along route A-B and during driving traverses along Fetveien, route C-D. Crosswind concentration profiles for traverses along the two routes are shown in Figures A2 and A3.

The wind speed averaged 2.2 m/s from 201° during the test. Atmospheric stability conditions were slightly unstable.

A.1.2 Test 2, 30 March 1978

SF_6 was released at 1 m above ground from point R1 from 1000 to 1045 at a rate of .0833 g/s. Crosswind concentration profiles, drawn from instantaneous data collected along lines A-B and C-D are shown in Figures A4 and A5. Fifteen minute average data from 2 points along Fetveien are also given.

The average wind speed during the test was 4.0 m/s from 207°. Atmospheric stability conditions were unstable.

A.1.3 Test 3, 12 May 1978

SF_6 was released at 1 m above ground from point R3 from 1410 to 1440 at a rate of .0833 g/s. Fifteen minute average samples were collected along lines A-B and E-F. The tracer data are shown in Figure A6.

Wind conditions during the test averaged 3.7 m/s from 105°. Atmospheric stability conditions were unstable.

A.1.4 Test 4, 6 June 1978

SF_6 was released at 1 m above ground from point R1 from 1652 to 1717 at a rate of .0881 g/s. Fifteen minute average data were collected along lines A-B and C-D. These data are shown in Figure A7. In addition, 15 minute average vertical profile data were collected with samples attached to the 10 m mast at point 5. These data are given in Figure A8.

Wind conditions during the test averaged 4.0 m/s from 206°. Atmospheric stability conditions were unstable.

A.1.5 Test 5, 7 June 1978

SF_6 was released at 1 m above ground from point R1 from 1430 to 1455 at a rate of .0829 g/s. Fifteen minute average data, collected along lines A-B and C-D, are shown in Figure A9. Vertical concentration data, collected at the 10-m mast, are shown in Figure A10.

Wind conditions during the test averaged 3.7 m/s from 199°. ATmospheric stability conditions were unstable.

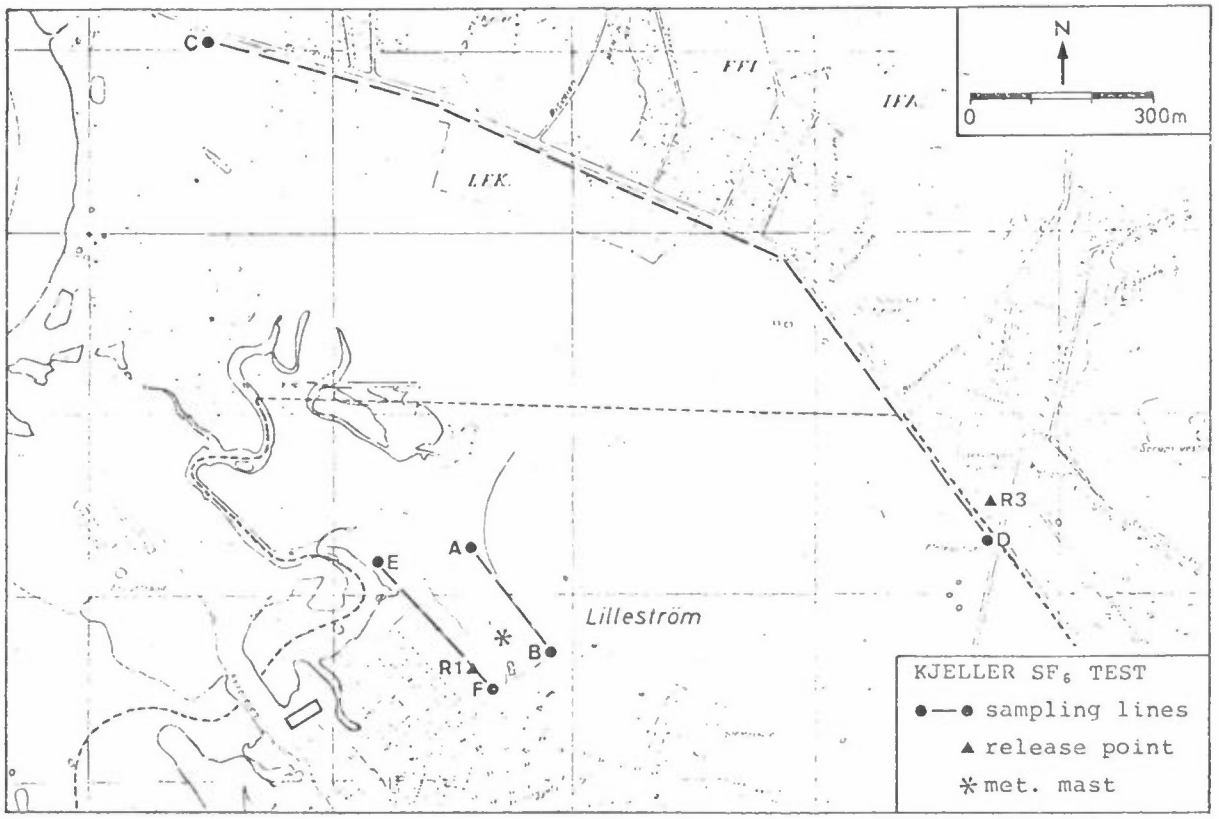

Figure A1: Map of site K.

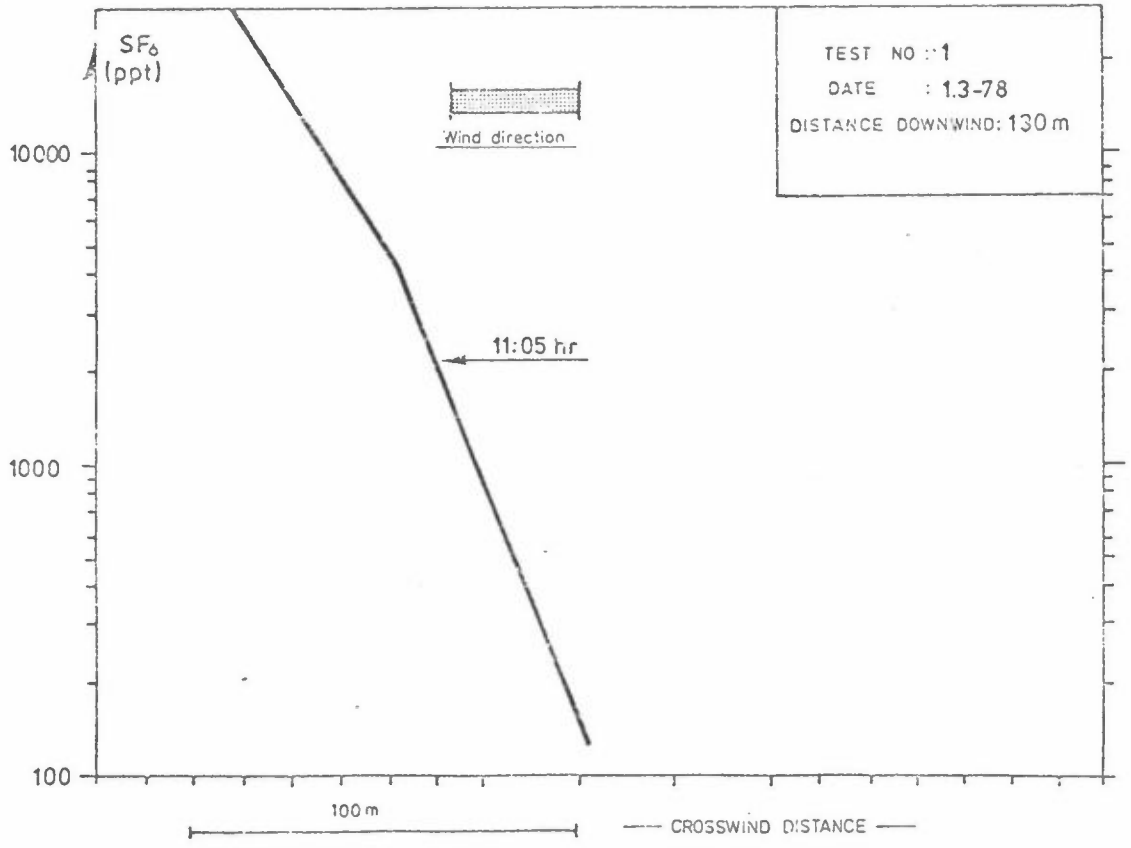

Figure A2: Crosswind instantaneous SF_6 concentration profile observed along sampling line A-B.

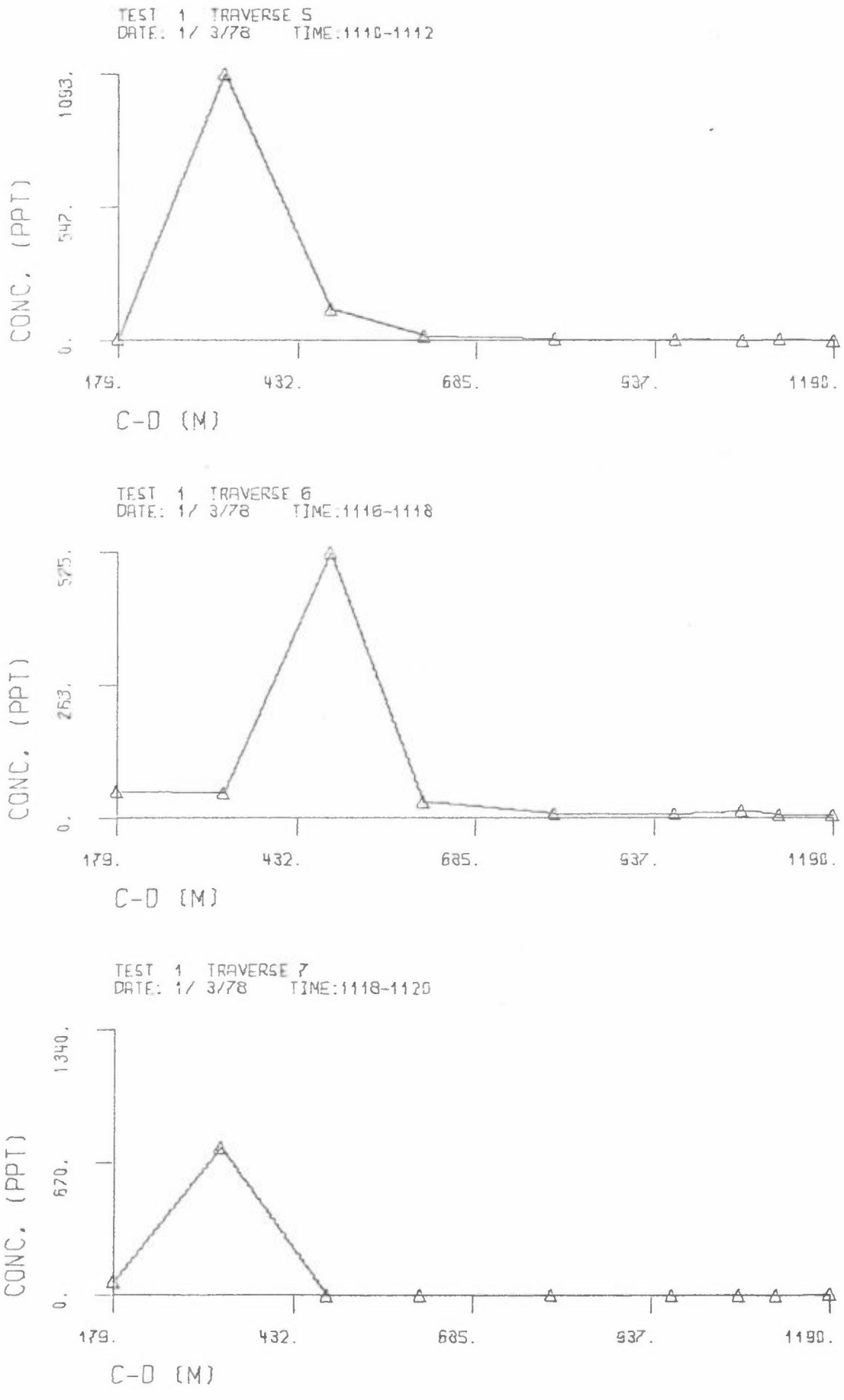

Figure A3: Crosswind instantaneous SF_6 concentration profiles observed along sampling line C-D.

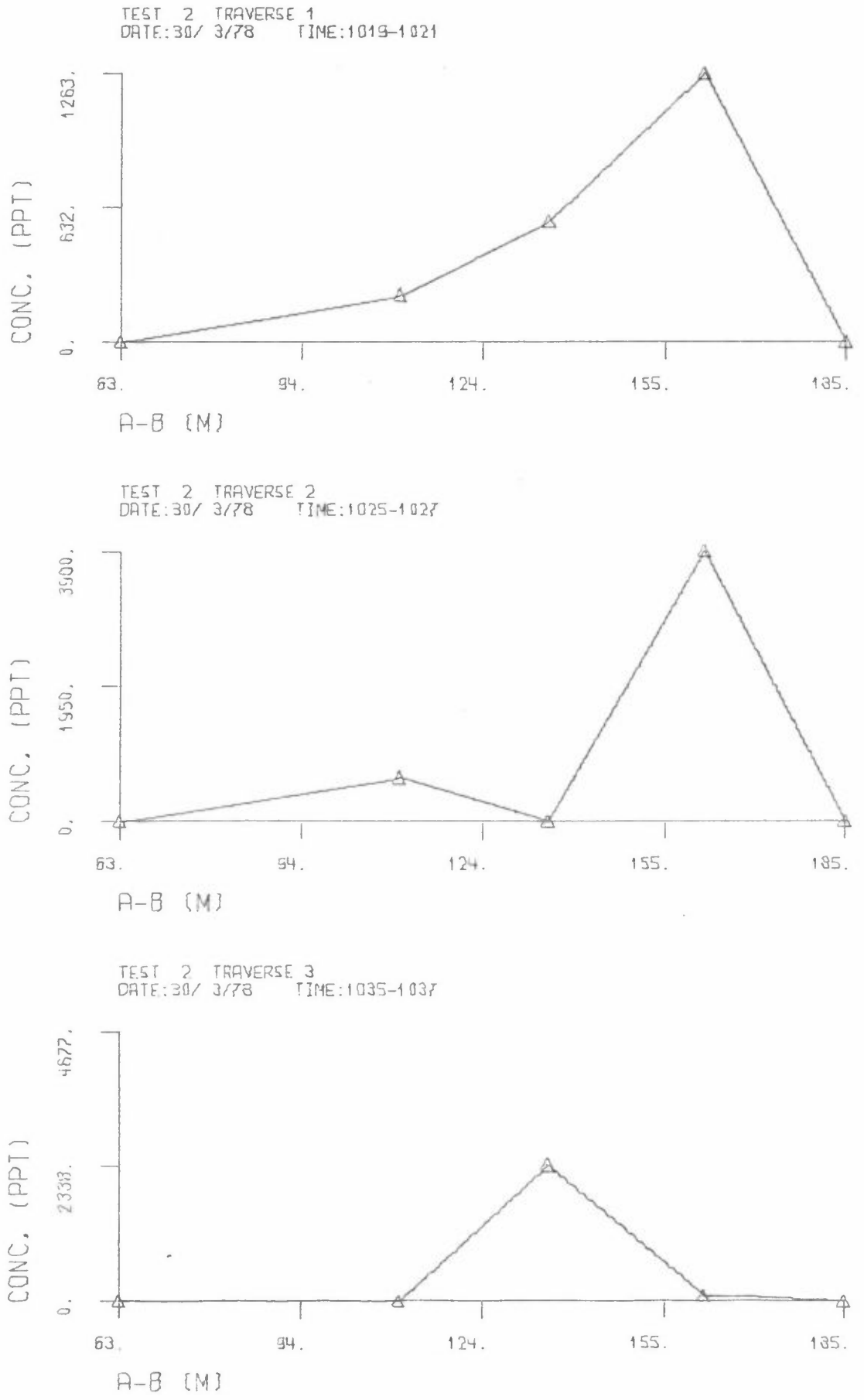

Figure A4: Crosswind instantaneous SF_6 concentration profiles observed along sampling line A-B.

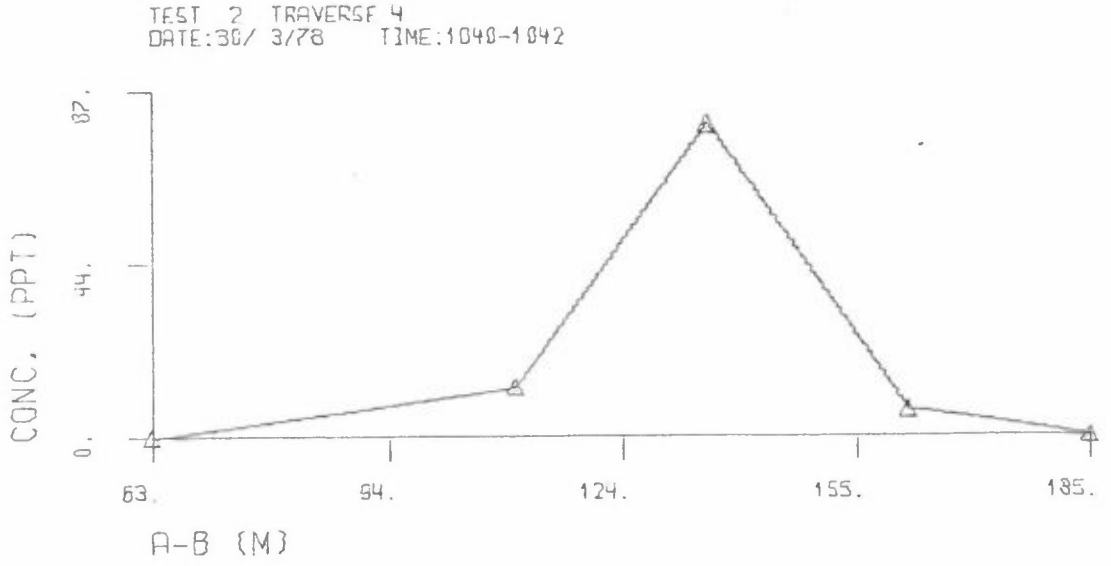

Figure A4: Crosswind instantaneous SF_6 concentration profiles observed along sampling line A-B.

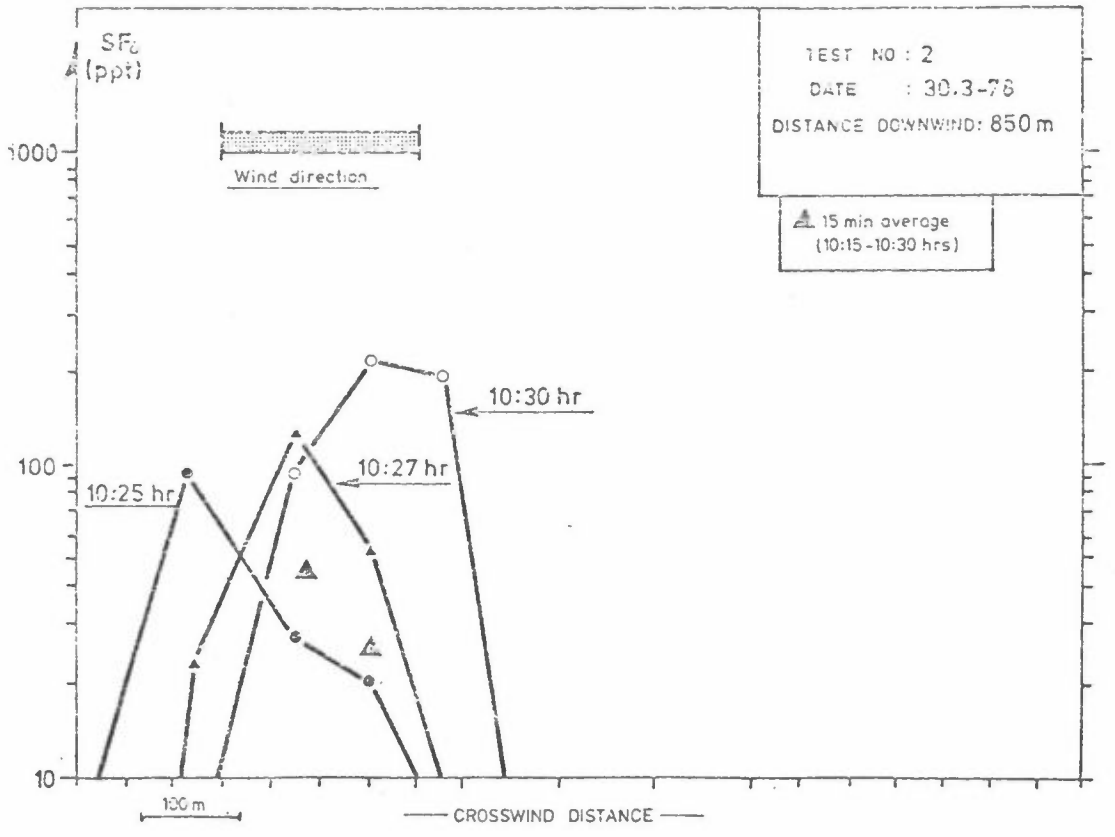

Figure A5: Crosswind instantaneous SF_6 concentration profiles observed along sampling line C-D.

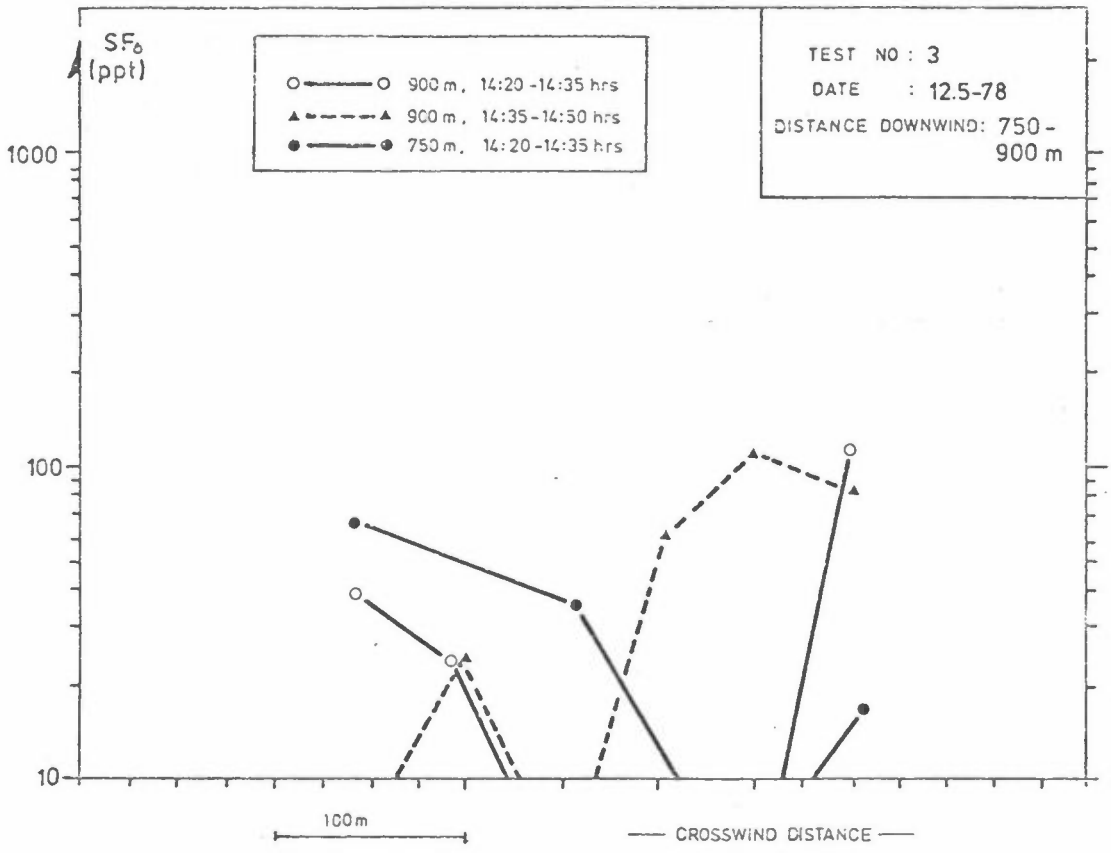

Figure A6: Fifteen-minute average SF_6 concentration profiles observed along sampling lines A-B and E-F.

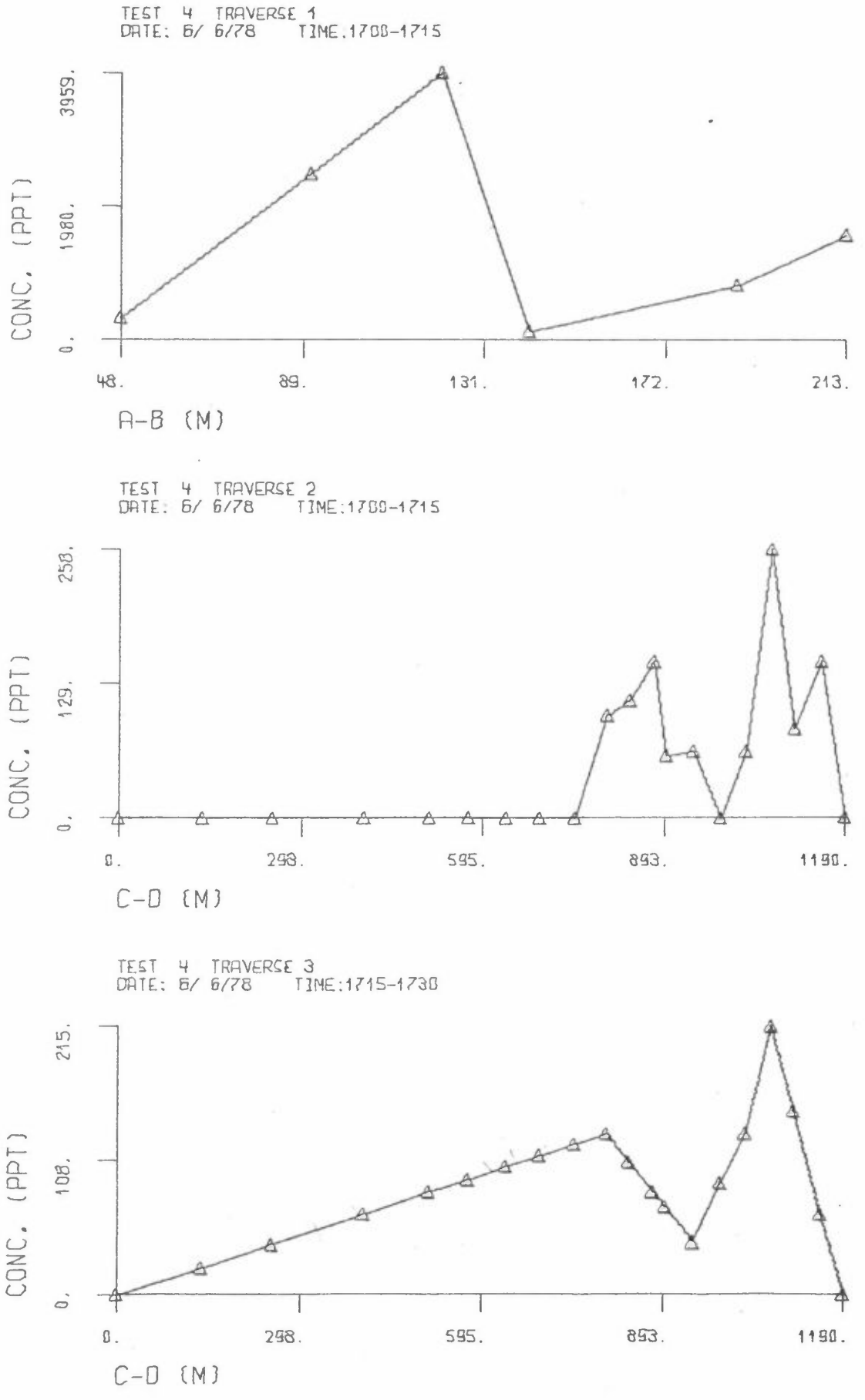

Figure A7: Crosswind 15-minute average SF_6 concentration profiles observed along sampling lines A-B and C-D.

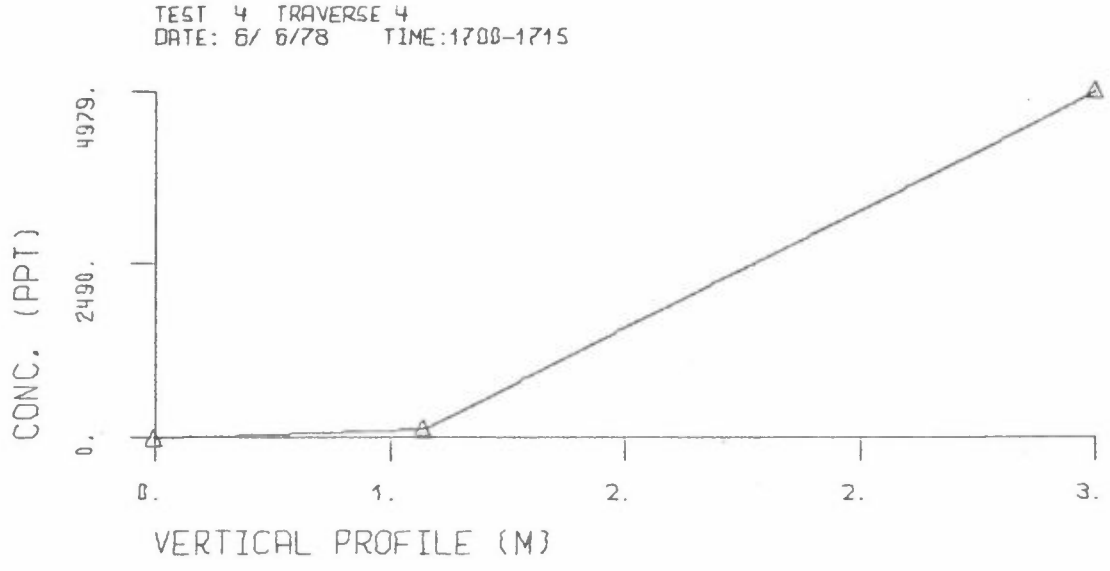

Figure A8: Vertical 15-minute average SF_6 concentration profile observed 70 m downwind.

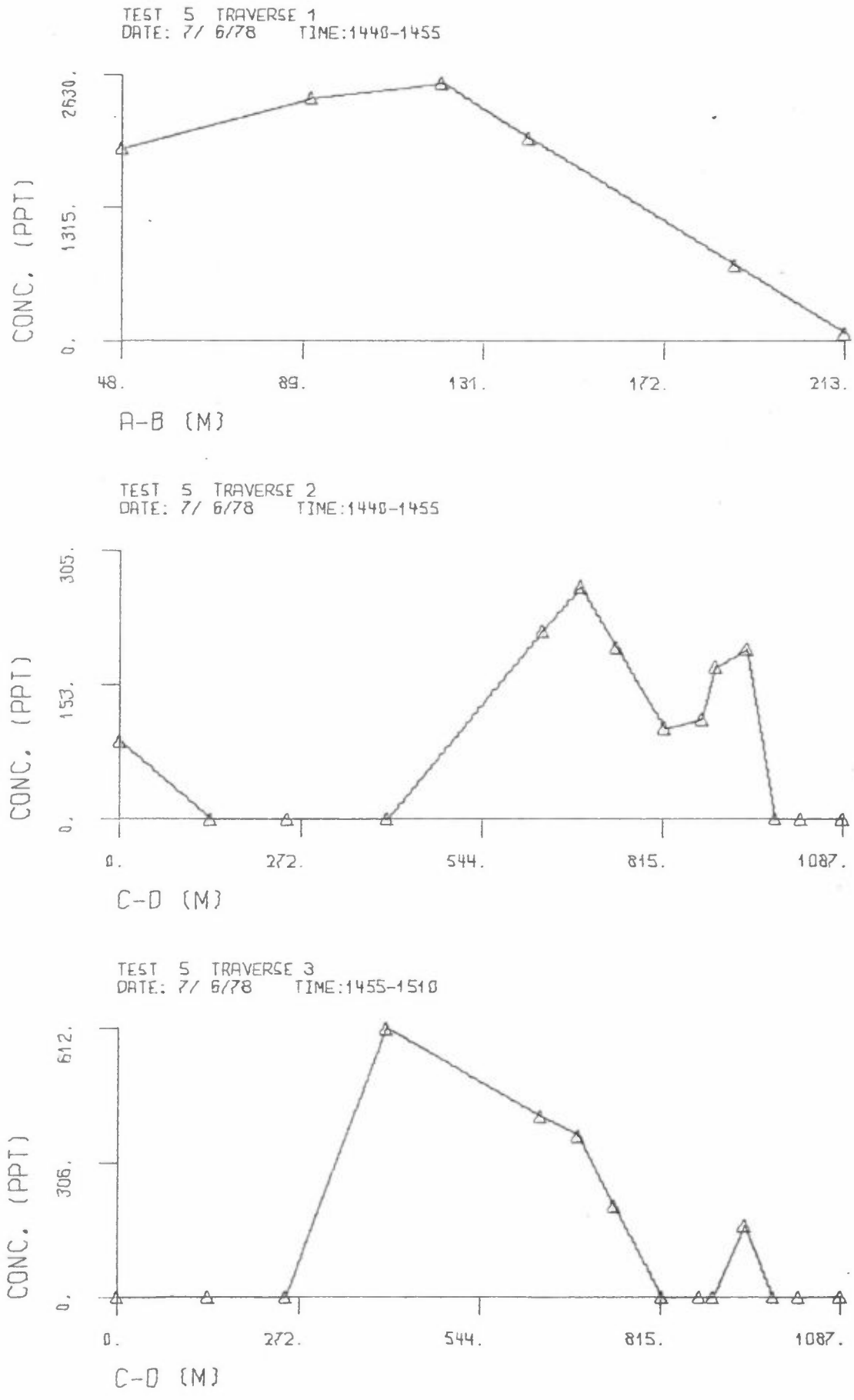

Figure A9: Crosswind 15-minute average SF_6 concentration profiles observed along sampling lines A-B and C-D.

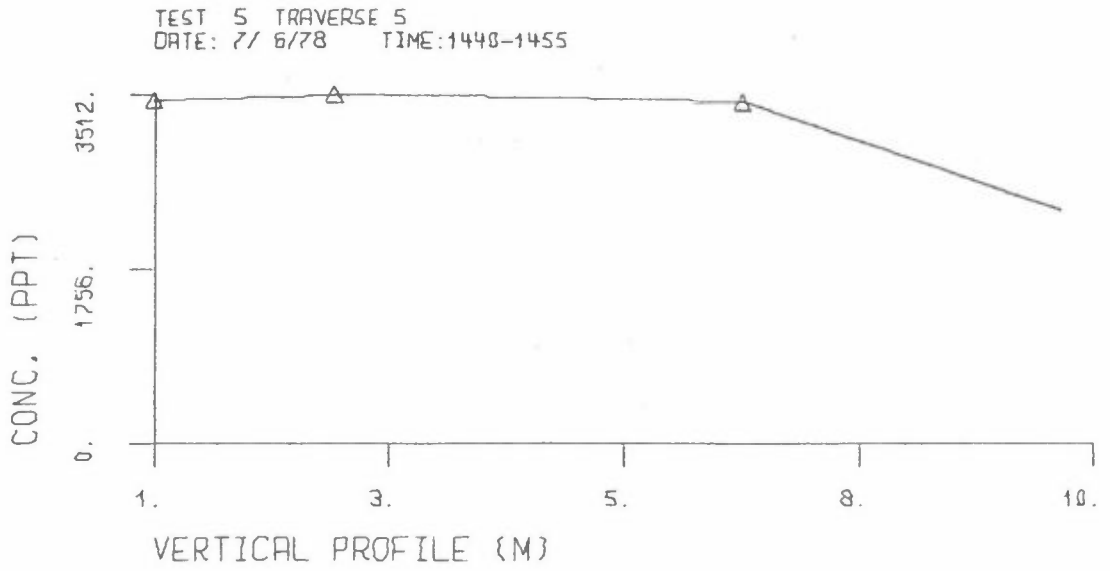

Figure A10: Vertical 15-minute average SF_6 concentration profile observed 70 m downwind.

Table A1: SF_6 Tracer Data, Site K.

TEST NO. 1
TRAVERSE NO. 2
TRAV. DESCRIPTION: A-B (M)
HEIGHT= 0.0 M
DISTANCE DOWNWIND= .13 KM
DATE: 1/ 3/78 TIME: 1105-1107

DISTANCE (M)	SF6 (PPT)
35.0	44216.
78.0	4900.
118.0	130.
155.0	11.
190.0	8.

TEST NO. 1
TRAVERSE NO. 5
TRAV. DESCRIPTION: C-D (M)
HEIGHT= 0.0 M
DISTANCE DOWNWIND= .85 KM
DATE: 1/ 3/78 TIME: 1110-1112

DISTANCE (M)	SF6 (PPT)
179.0	8.
329.0	1093.
479.0	129.
612.0	16.
796.0	8.
966.0	6.
1060.0	2.
1114.0	8.
1190.0	0.

TEST NO. 1
TRAVERSE NO. 6
TRAV. DESCRIPTION: C-D (M)
HEIGHT= 0.0 M
DISTANCE DOWNWIND= .85 KM
DATE: 1/ 3/78 TIME: 1116-1118

DISTANCE (M)	SF6 (PPT)
179.0	52.
329.0	50.
479.0	525.
612.0	33.
796.0	8.
966.0	10.
1060.0	14.
1114.0	6.
1190.0	7.

TEST NO. 1
TRAVERSE NO. 7
TRAV. DESCRIPTION: C-D (M)
HEIGHT= 0.0 M
DISTANCE DOWNWIND= .85 KM
DATE: 1/ 3/78 TIME: 1118-1120

DISTANCE (M)	SF6 (PPT)
179.0	68.
329.0	738.
479.0	2.
612.0	0.
796.0	0.
966.0	0.
1060.0	0.
1114.0	0.
1190.0	5.

Table A1: Continued

TEST NO. 2
TRAVERSE NO. 5
TRAV. DESCRIPTION: C-D (M)
HEIGHT= 0.0 M
DISTANCE DOWNWIND= .85 KM
DATE: 30/ 3/78 TIME: 1025-1026

DISTANCE (M)	SF6 (PPT)
662.0	0.
789.0	97.
907.0	29.
971.0	25.
1055.0	0.
1160.0	0.
1271.0	0.
1339.0	0.

TEST NO. 2
TRAVERSE NO. 6
TRAV. DESCRIPTION: C-D (M)
HEIGHT= 0.0 M
DISTANCE DOWNWIND= .85 KM
DATE: 30/ 3/78 TIME: 1027-1028

DISTANCE (M)	SF6 (PPT)
662.0	0.
789.0	0.
907.0	23.
971.0	54.
1055.0	0.
1160.0	0.
1271.0	0.
1339.0	0.

TEST NO. 2
TRAVERSE NO. 7
TRAV. DESCRIPTION: C-D (M)
HEIGHT= 0.0 M
DISTANCE DOWNWIND= .85 KM
DATE: 30/ 3/78 TIME: 1030-1031

DISTANCE (M)	SF6 (PPT)
662.0	0.
789.0	0.
907.0	94.
971.0	219.
1055.0	191.
1160.0	0.
1271.0	0.
1339.0	0.

Table A1: Cont.

TEST NO. 2
TRAVERSE NO. 1
TRAV. DESCRIPTION: A-B (M)
HEIGHT= 0.0 M
DISTANCE DOWNWIND= .13 KM
DATE: 30/ 3/78 TIME: 1019-1021

DISTANCE (M)	SF6 (PPT)
63.0	0.
110.0	224.
135.0	570.
161.0	1263.
185.0	0.

TEST NO. 2
TRAVERSE NO. 2
TRAV. DESCRIPTION: A-B (M)
HEIGHT= 0.0 M
DISTANCE DOWNWIND= .13 KM
DATE: 30/ 3/78 TIME: 1025-1027

DISTANCE (M)	SF6 (PPT)
63.0	0.
110.0	649.
135.0	0.
161.0	3900.
185.0	0.

TEST NO. 2
TRAVERSE NO. 3
TRAV. DESCRIPTION: A-B (M)
HEIGHT= 0.0 M
DISTANCE DOWNWIND= .13 KM
DATE: 30/ 3/78 TIME: 1035-1037

DISTANCE (M)	SF6 (PPT)
63.0	0.
110.0	0.
135.0	2374.
161.0	115.
185.0	0.

TEST NO. 2
TRAVERSE NO. 4
TRAV. DESCRIPTION: A-B (M)
HEIGHT= 0.0 M
DISTANCE DOWNWIND= .13 KM
DATE: 30/ 3/78 TIME: 1040-1042

DISTANCE (M)	SF6 (PPT)
63.0	0.
110.0	13.
135.0	79.
161.0	7.
185.0	0.

Table A1: Cont.

TEST NO. 3
TRAVERSE NO. 1
TRAV. DESCRIPTION: B-A (M)
HEIGHT= 0.0 M
DISTANCE DOWNWIND= .77 KM
DATE: 12/ 5/78 TIME: 1410-1425

DISTANCE (M)	SF6 (PPT)
20.0	19.
68.0	0.
123.0	38.
218.0	63.

TEST NO. 3
TRAVERSE NO. 2
TRAV. DESCRIPTION: B-A (M)
HEIGHT= 0.0 M
DISTANCE DOWNWIND= .77 KM
DATE: 12/ 5/78 TIME: 1425-1440

DISTANCE (M)	SF6 (PPT)
20.0	0.
68.0	0.
123.0	57.
218.0	-1.

TEST NO. 3
TRAVERSE NO. 3
TRAV. DESCRIPTION: F-E (M)
HEIGHT= 0.0 M
DISTANCE DOWNWIND= .92 KM
DATE: 12/ 5/78 TIME: 1410-1425

DISTANCE (M)	SF6 (PPT)
90.0	113.
113.0	0.
155.0	0.
193.0	0.
230.0	25.
290.0	38.

TEST NO. 3
TRAVERSE NO. 4
TRAV. DESCRIPTION: F-E (M)
HEIGHT= 0.0 M
DISTANCE DOWNWIND= .92 KM
DATE: 12/ 5/78 TIME: 1425-1440

DISTANCE (M)	SF6 (PPT)
90.0	88.
113.0	107.
155.0	63.
193.0	0.
230.0	25.
290.0	0.

Table A1: Cont.

TEST NO. 4
TRAVERSE NO. 1
TRAV. DESCRIPTION: A-B (M)
HEIGHT= 0.0 M
DISTANCE DOWNWIND= .13 KM
DATE: 6/ 6/78 TIME: 1700-1715

DISTANCE (M)	SF6 (PPT)
48.0	343.
91.0	2468.
121.0	3959.
141.0	129.
188.0	794.
213.0	1575.

TEST NO. 4
TRAVERSE NO. 2
TRAV. DESCRIPTION: C-D (M)
HEIGHT= 0.0 M
DISTANCE DOWNWIND= .85 KM
DATE: 6/ 6/78 TIME: 1700-1715

DISTANCE (M)	SF6 (PPT)	DISTANCE (M)	SF6 (PPT)
0.0	-1.	1025.0	64.
135.0	-1.	1068.0	258.
250.0	-1.	1105.0	86.
400.0	-1.	1150.0	150.
510.0	0.	1190.0	0.
573.0	0.		
635.0	0.		
690.0	-1.		
745.0	0.		
798.0	99.		
835.0	113.		
875.0	150.		
895.0	59.		
940.0	64.		
985.0	0.		

TEST NO. 4
TRAVERSE NO. 3
TRAV. DESCRIPTION: C-D (M)
HEIGHT= 0.0 M
DISTANCE DOWNWIND= .85 KM
DATE: 6/ 6/78 TIME: 1715-1730

DISTANCE (M)	SF6 (PPT)	DISTANCE (M)	SF6 (PPT)
0.0	-1.	1025.0	129.
135.0	-1.	1068.0	215.
250.0	-1.	1105.0	-1.
400.0	-1.	1150.0	64.
510.0	-1.	1190.0	-1.
573.0	-1.		
635.0	-1.		
690.0	-1.		
745.0	-1.		
798.0	129.		
835.0	-1.		
875.0	-1.		
895.0	-1.		
940.0	43.		
985.0	90.		

TEST NO. 4
TRAVERSE NO. 4
TRAV. DESCRIPTION: VERTICAL PROFILE (M)
HEIGHT= 0.0 M
DISTANCE DOWNWIND= .07 KM
DATE: 6/ 6/78 TIME: 1700-1715

DISTANCE (M)	SF6 (PPT)
.2	0.
1.0	129.
3.0	4979.

Table A1: Cont.

TEST NO. 5
TRAVERSE NO. 1
TRAV. DESCRIPTION: A-B (M)
HEIGHT= 0.0 M
DISTANCE DOWNWIND= .13 KM
DATE: 7/ 6/78 TIME: 1440-1455

DISTANCE (M)	SF6 (PPT)
48.0	1901.
91.0	2388.
121.0	2532.
141.0	-1.
188.0	1321.
213.0	77.

TEST NO. 5
TRAVERSE NO. 2
TRAV. DESCRIPTION: C-D (M)
HEIGHT= 0.0 M
DISTANCE DOWNWIND= .85 KM
DATE: 7/ 6/78 TIME: 1440-1455

DISTANCE (M)	SF6 (PPT)
0.0	87.
135.0	0.
250.0	0.
400.0	0.
635.0	-1.
690.0	264.
745.0	-1.
817.0	103.
875.0	113.
895.0	172.
940.0	193.
985.0	0.
1025.0	0.
1087.0	0.

TEST NO. 5
TRAVERSE NO. 3
TRAV. DESCRIPTION: C-D (M)
HEIGHT= 0.0 M
DISTANCE DOWNWIND= .85 KM
DATE: 7/ 6/78 TIME: 1455-1510

DISTANCE (M)	SF6 (PPT)
0.0	-1.
135.0	-1.
250.0	0.
400.0	612.
635.0	-1.
690.0	365.
745.0	-1.
810.0	0.
875.0	0.
895.0	0.
940.0	161.
985.0	0.
1025.0	-1.
1087.0	0.

TEST NO. 5
TRAVERSE NO. 4
TRAV. DESCRIPTION: CK-FK (M)
HEIGHT= 0.0 M
DISTANCE DOWNWIND= 2.00 KM
DATE: 7/ 6/78 TIME: 1440-1455

DISTANCE (M)	SF6 (PPT)
0.0	122.
350.0	0.
700.0	0.
1050.0	0.

TEST NO. 5
TRAVERSE NO. 5
TRAV. DESCRIPTION: VERTICAL PROFILE (M)
HEIGHT= 0.0 M
DISTANCE DOWNWIND= .07 KM
DATE: 7/ 6/78 TIME: 1440-1455

DISTANCE (M)	SF6 (PPT)
.7	3448.
2.5	3512.
6.5	3434.
10.0	2223.

A.2 Site V

A map of site V is shown in Figure A11. It is a rocky coastal site with little vegetation. The surface roughness is estimated to be .4 m. The tracer data are tabulated in Table A2.

A.2.1 Test 6, 29 May 1978

SF_6 was released at 1 m above ground from the base of the 36 m mast from 1255 to 1335 at a rate of .0728 g/s. Fifteen minute average data were collected along two arcs; these data are given in Figures A12 and A13.

Wind conditions during the test averaged 3.8 m/s from 236° at 10 m. Conditions observed at 36 m averaged 4.2 m/s from 250°. Atmospheric stability conditions were unstable.

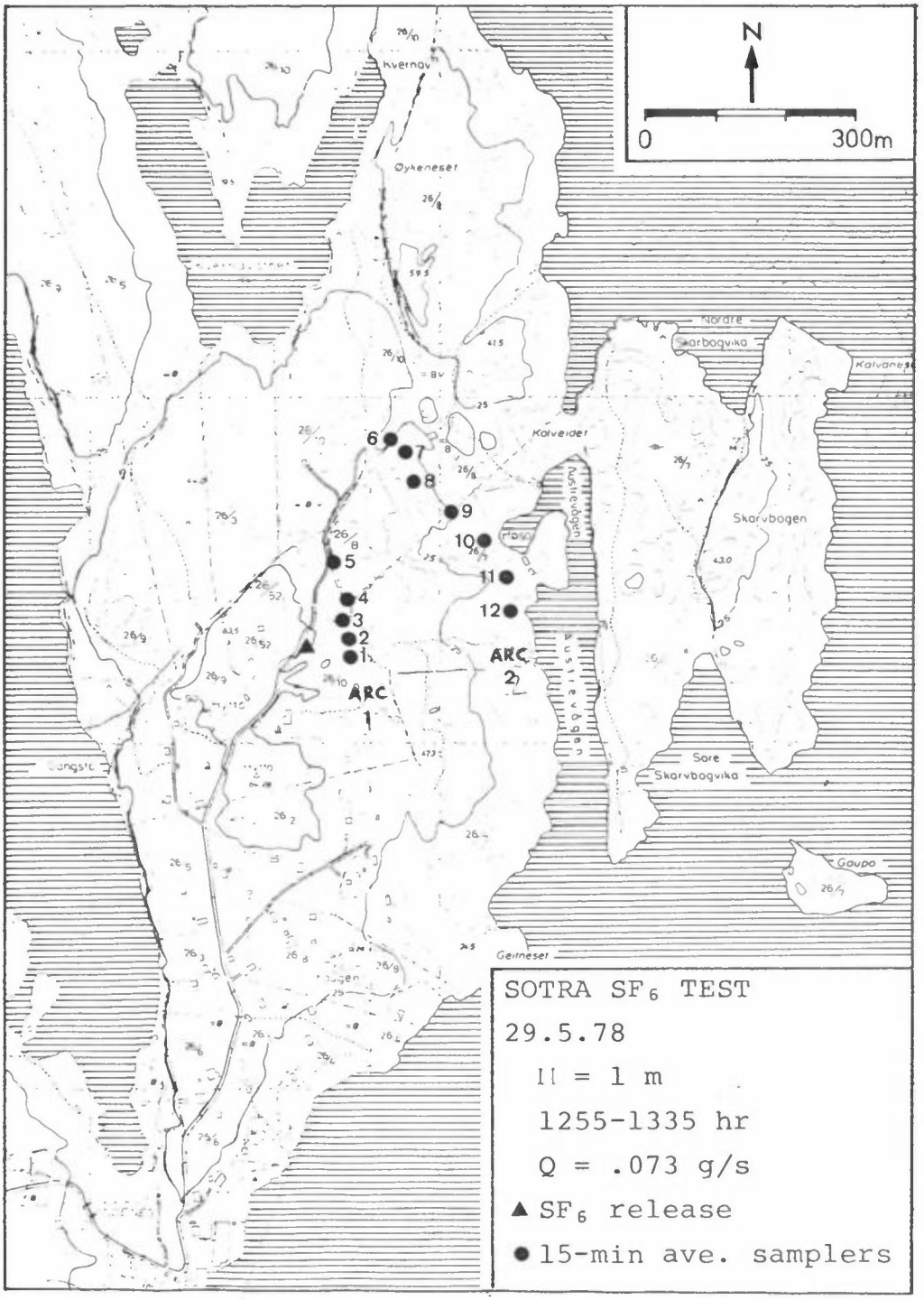

Figure A11: Map of site V.

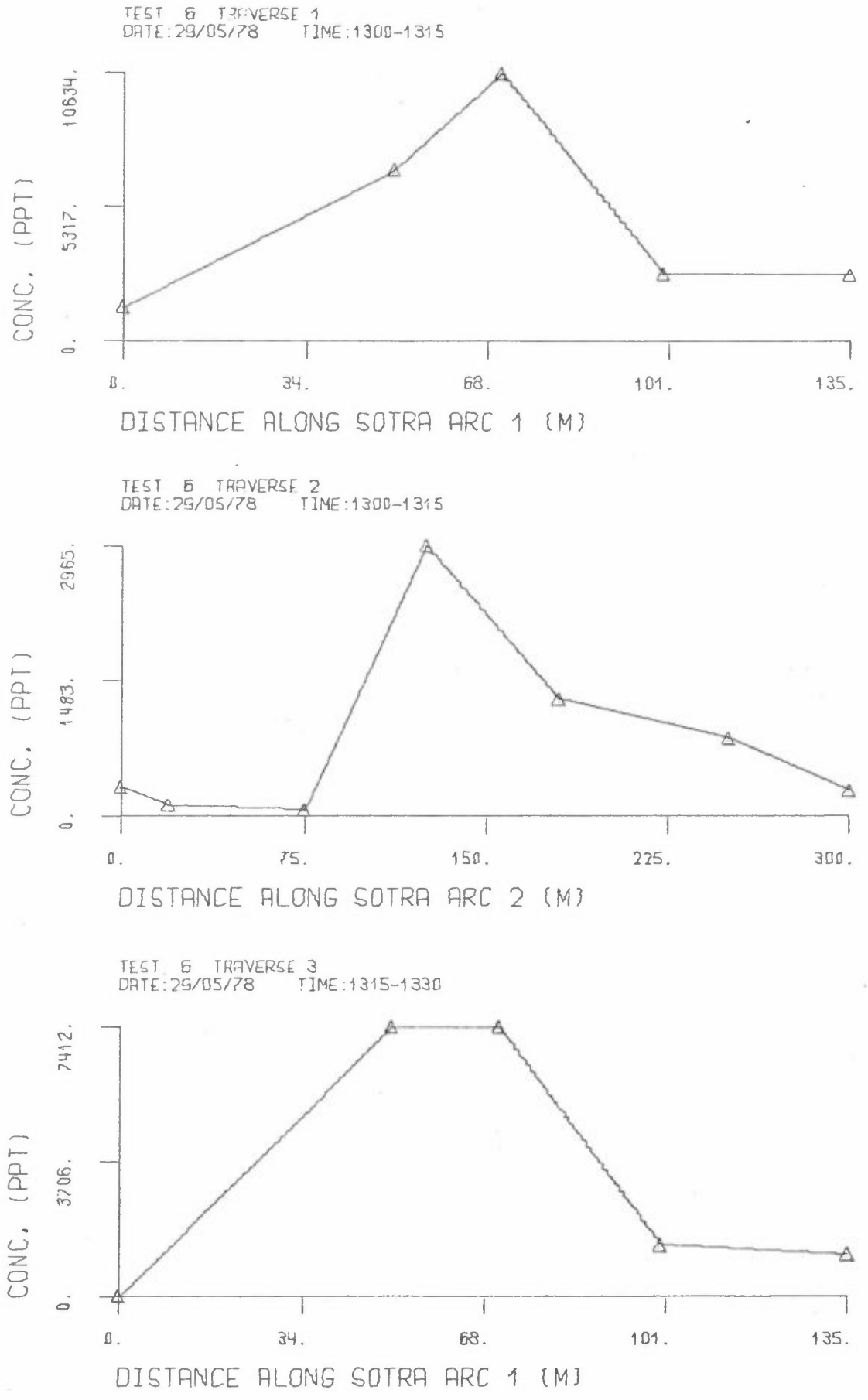

Figure A12: Crosswind 15-minute average SF_6 concentration profiles observed 100 m and 300 m downwind.

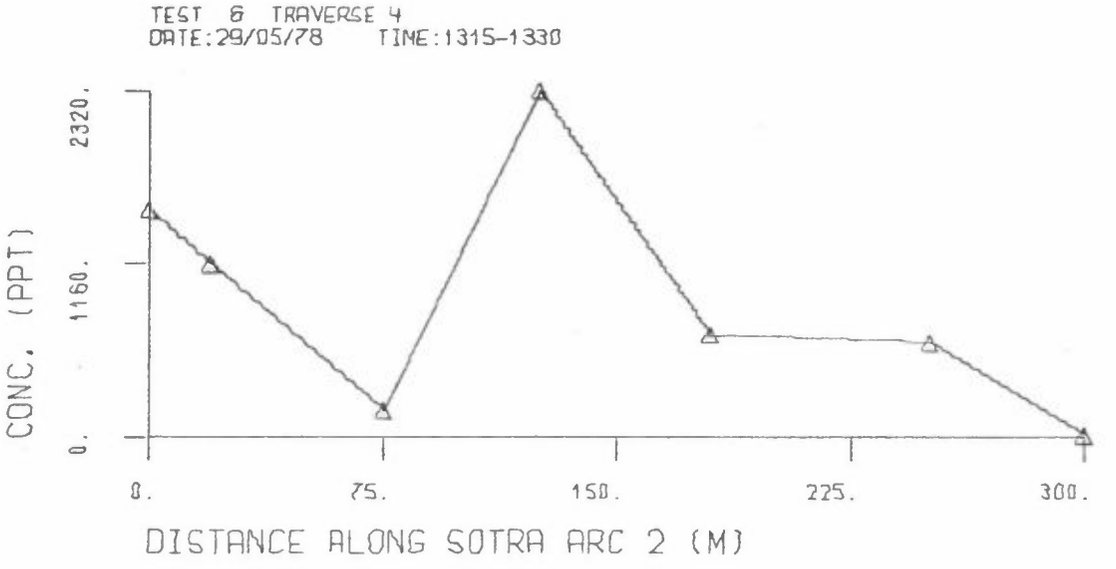

Figure A13: Crosswind 15-minute average SF_6 concentration profile observed 300 m downwind.

Table A2: SF_6 Tracer Data, Site V.

TEST NO. 1 SOTRA
TRAVERSE NO. 1
TRAV. DESCRIPTION: DISTANCE ALONG SOTRA ARC 1 (M)
HEIGHT= 0.0 M
DISTANCE DOWNWIND= .10 KM
DATE: 29/05/78 TIME: 1300-1315

DISTANCE (M)	SF6 (PPT)
0.0	1353.
50.0	6767.
70.0	10634.
100.0	2642.
135.0	2610.

TEST NO. 1
TRAVERSE NO. 2
TRAV. DESCRIPTION: DISTANCE ALONG SOTRA ARC 2 (M)
HEIGHT= 0.0 M
DISTANCE DOWNWIND= .30 KM
DATE: 29/05/78 TIME: 1300-1315

DISTANCE (M)	SF6 (PPT)
0.0	322.
20.0	116.
75.0	64.
125.0	2965.
180.0	1289.
250.0	854.
300.0	280.

TEST NO. 1
TRAVERSE NO. 3
TRAV. DESCRIPTION: DISTANCE ALONG SOTRA ARC 1 (M)
HEIGHT= 0.0 M
DISTANCE DOWNWIND= .10 KM
DATE: 29/05/78 TIME: 1315-1330

DISTANCE (M)	SF6 (PPT)
0.0	-1.
50.0	7412.
70.0	7412.
100.0	1434.
135.0	1192.

TEST NO. 1
TRAVERSE NO. 4
TRAV. DESCRIPTION: DISTANCE ALONG SOTRA ARC 2 (M)
HEIGHT= 0.0 M
DISTANCE DOWNWIND= .30 KM
DATE: 29/05/78 TIME: 1315-1330

DISTANCE (M)	SF6 (PPT)
0.0	1515.
20.0	-1.
75.0	184.
125.0	2320.
180.0	677.
250.0	628.
300.0	16.

A.3 Site A

A map of site A is given in Figure A14. It is an agricultural area of rolling hills interspersed with forested areas. The surface roughness is estimated to be .5 m. The data for site A are tabulated in Table A3.

A.3.1 Test 7, 26 July 1978

SF_6 was released from 40 m above the ground and 10 m above the roof of a silo located at the A/S Glassvatt in Askim. The release time and rate were 1000 to 1030 and 0.191 g/s, respectively. Fifteen minute average data were collected along routes A and B. Instantaneous samples were taken during automobile traverses along route B. As the data in Table A3 indicate, very little SF_6 was observed along route B. Data obtained along route A are shown in Figure A15.

Wind conditions averaged 1.6 m/s from 210°. Atmospheric stability conditions were unstable.

A.3.2 Test 8, 26 July 1978

SF_6 was released between 1300 and 1330 from the same location and at the same rate as in test 7. Significant SF_6 concentrations were observed along route A; these data are shown in Figure A15.

Wind conditions during this period averaged 2.0 m/s from 195°. Atmospheric stability conditions were unstable.

A.3.3 Test 9, 26 July 1978

SF_6 was released between 1600 and 1645 from the same location and at the same rate as in test 7. The data collected along route A are shown in Figure A15.

Wind conditions during the test averaged 1.8 m/s from 210°. Atmospheric stability conditions were unstable.

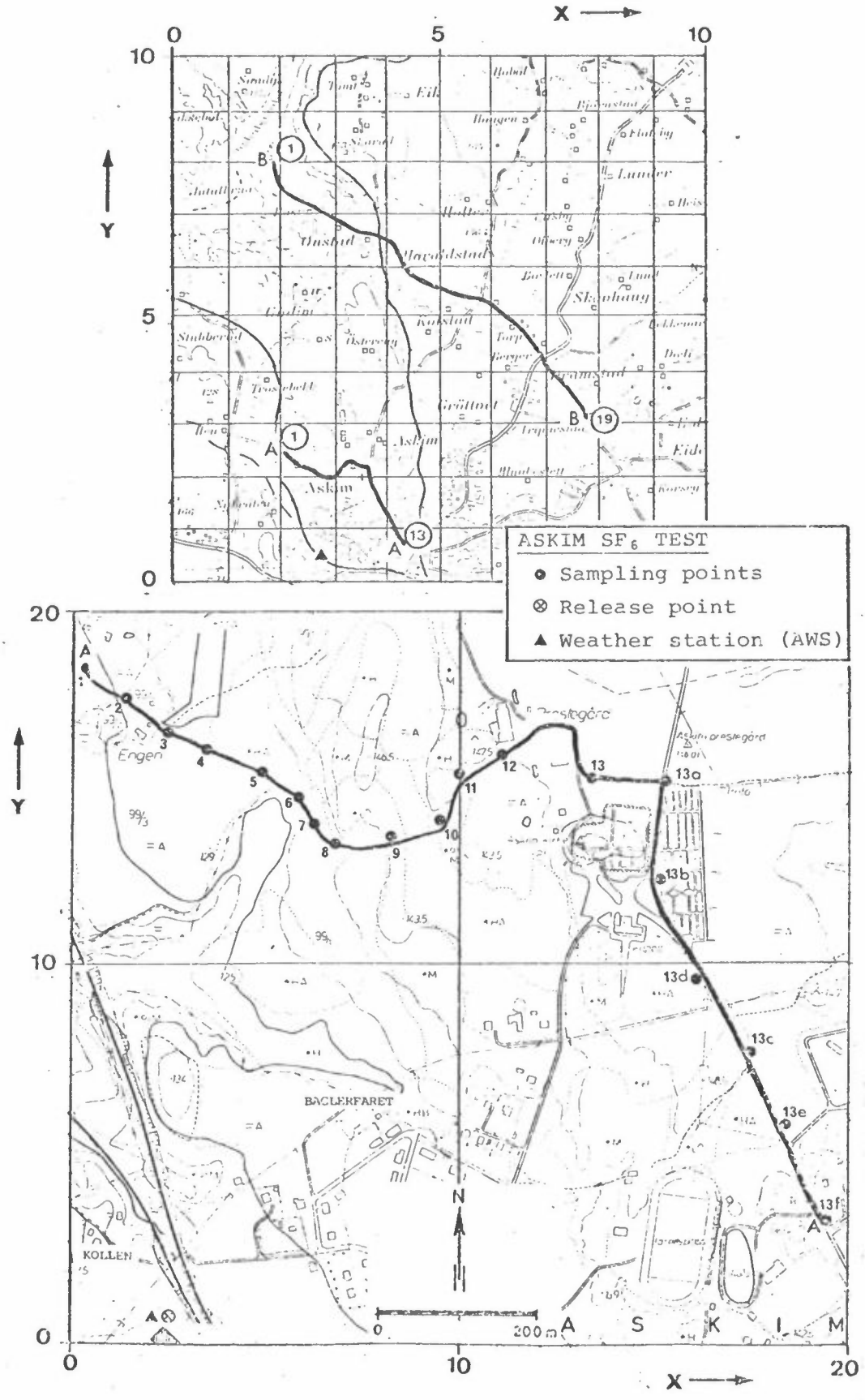

Figure A14: Map of site A.

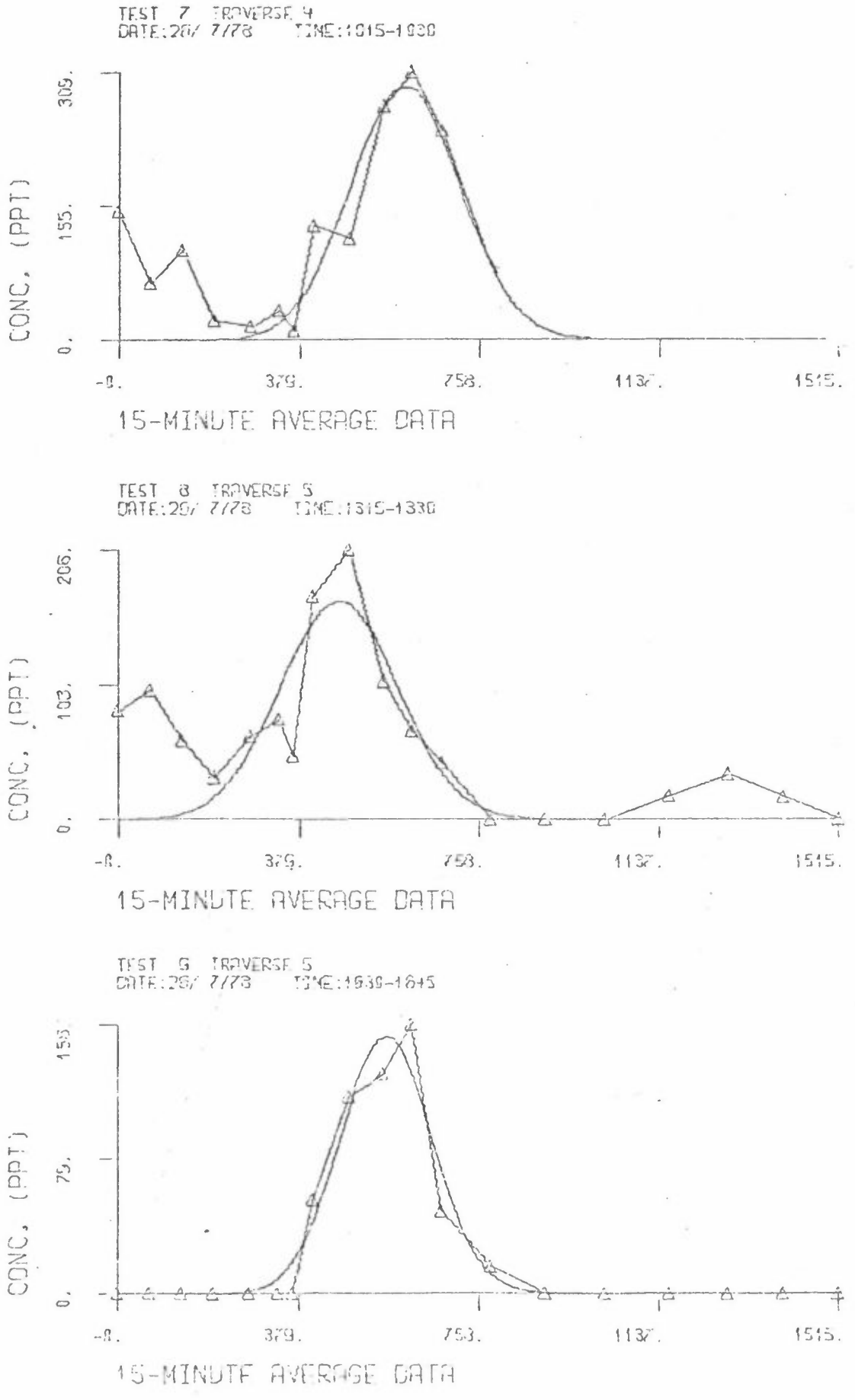

Figure A15: Crosswind 15-minute average SF_6 concentration profiles observed along sampling line A.

Table A3: SF_6 Tracer Data, Site A.

TEST NO. 7
DATA SET NO. 1
DESCRIPTION: 15-MINUTE AVERAGE DATA
SAMPLING HEIGHT(M) 1.0
GRID SCALE (M) 500
DATE: 26/ 7/78 TIME: 1015-1030

GRID COOR (X)	(Y)	SF6 (PPT)	GRID COOR (X)	(Y)	SF6 (PPT)	GRID COOR (X)	(Y)	SF6 (PPT)
2.6	3.0	148.	4.2	2.2	-1.	5.5	6.1	0
2.7	2.9	64.	4.4	2.0	-1.	6.0	5.9	16
2.9	2.7	103.	4.6	1.8	-1.	6.6	5.8	32
3.0	2.7	23.	4.7	1.5	-1.	6.9	5.6	0
3.1	2.6	16.	2.4	8.5	0.	7.1	5.4	0
3.2	2.6	35.	2.5	8.0	0.	7.3	5.2	0
3.3	2.5	10.	2.6	7.9	0.	7.4	4.9	0
3.4	2.5	132.	2.9	7.8	0.	7.8	4.4	-1
3.5	2.5	116.	3.0	7.1	0.	8.0	4.1	-1.
3.6	2.6	271.	3.2	7.6	13	8.3	3.7	-1
3.7	2.7	309.	3.5	7.5	0.			
3.8	2.8	242.	3.7	7.3	32.			
4.0	2.7	84.	4.1	7.2	0.			
4.2	2.7	-1.	4.5	7.1	0.			
4.2	2.4	-1.	4.8	6.5	0.			

TEST NO. 7
DATA SET NO. 2
DESCRIPTION: B1-B18
SAMPLING HEIGHT(M) 1.0
GRID SCALE (M) 500.
DATE: 26/ 7/78 TIME: 1015-1029

GRID COOR (X)	(Y)	SF6 (PPT)	GRID COOR (X)	(Y)	SF6 (PPT)
2.4	8.5	0.	7.1	5.4	0.
2.5	8.0	0.	7.3	5.2	0.
2.6	7.9	0.	7.4	4.9	0.
2.9	7.8	0.			
3.0	7.7	0.			
3.2	7.6	0.			
3.5	7.5	0.			
3.7	7.3	0.			
4.1	7.2	0.			
4.5	7.1	0.			
4.8	6.5	0.			
5.5	6.1	0.			
6.0	5.9	0.			
6.6	5.8	0.			
6.9	5.6	0.			

TEST NO. 7
DATA SET NO. 3
DESCRIPTION: B1-B18
SAMPLING HEIGHT(M) 1.0
GRID SCALE (M) 500.
DATE: 26/ 7/78 TIME: 1030-1035

GRID COOR (X)	(Y)	SF6 (PPT)	GRID COOR (X)	(Y)	SF6 (PPT)
2.4	8.5	0.	7.1	5.4	0.
2.5	8.0	0.	7.3	5.2	0.
2.6	7.9	0.	7.4	4.9	0.
2.9	7.8	0.			
3.0	7.7	0.			
3.2	7.6	0.			
3.5	7.5	0.			
3.7	7.3	0.			
4.1	7.2	0.			
4.5	7.1	0.			
4.8	6.5	0.			
5.5	6.1	0.			
6.0	5.9	0.			
6.6	5.8	0.			
6.9	5.6	0.			

TEST NO. 7
DATA SET NO. 4
DESCRIPTION: 15-MINUTE AVERAGE DATA
SAMPLING HEIGHT(M) 1.0
GRID SCALE (M) 50.
DATE: 26/ 7/78 TIME: 1015-1030

GRID COOR (X)	(Y)	SF6 (PPT)	GRID COOR (X)	(Y)	SF6 (PPT)
.8	18.4	148.	16.6	10.3	-1.
1.8	17.5	64.	17.9	8.2	-1.
2.8	16.7	103.	18.9	6.1	-1.
4.0	16.1	23.	19.9	4.0	-1.
5.4	15.5	16.			
6.4	14.9	35.			
6.7	14.3	10.			
7.3	13.7	132.			
8.8	13.7	116.			
10.1	14.2	271.			
10.5	15.4	309.			
11.6	16.0	242.			
13.6	15.4	84.			
15.9	15.3	-1.			
15.6	12.8	-1.			

Table A3: Cont.

TEST NO. 8
DATA SET NO. 1
DESCRIPTION: 15-MINUTE AVERAGE DATA
SAMPLING HEIGHT(M) 1.0
GRID SCALE (M) 500.
DATE: 26/ 7/78 TIME: 1315-1330

GRID COOR (X)	(Y)	SF6 (PPT)	GRID COOR (X)	(Y)	SF6 (PPT)	GRID COOR (X)	(Y)	SF6 (PPT)
2.6	3.0	84.	4.2	2.2	-1.	5.5	6.1	106
2.7	2.9	100.	4.4	2.0	35.	6.0	5.9	0
2.9	2.7	61.	4.6	1.8	-1.	6.6	5.8	0
3.0	2.7	32.	4.7	1.5	-1.	6.9	5.6	0
3.1	2.6	64.	2.4	8.5	0.	7.1	5.4	232
3.2	2.6	77.	2.5	8.0	0.	7.3	5.2	0
3.3	2.5	48.	2.6	7.9	0.	7.4	4.9	287
3.4	2.5	171.	2.9	7.8	0.	7.8	4.4	-1
3.5	2.5	206.	3.0	7.7	0.	8.0	4.1	-1
3.6	2.6	106.	3.2	7.6	10.	8.3	3.7	-1
3.7	2.7	68.	3.5	7.5	16.			
3.8	2.8	-1.	3.7	7.3	16.			
4.0	2.7	0.	4.1	7.2	0.			
4.2	2.7	0.	4.5	7.1	0.			
4.2	2.4	0.	4.8	6.5	0.			

TEST NO. 8
DATA SET NO. 2
DESCRIPTION: B1-B18
SAMPLING HEIGHT(M) 1.0
GRID SCALE (M) 500.
DATE: 26/ 7/78 TIME: 1312-1322

GRID COOR (X)	(Y)	SF6 (PPT)	GRID COOR (X)	(Y)	SF6 (PPT)
2.4	8.5	0.	7.1	5.4	0.
2.5	8.0	0.	7.3	5.2	0.
2.6	7.9	0.	7.4	4.9	0.
2.9	7.8	0.			
3.0	7.7	0.			
3.2	7.6	0.			
3.5	7.5	0.			
3.7	7.3	0.			
4.1	7.2	0.			
4.5	7.1	0.			
4.8	6.5	0.			
5.5	6.1	0.			
6.0	5.9	0.			
6.6	5.8	0.			
6.9	5.6	0.			

Table A3: Cont.

TEST NO. 8
DATA SET NO. 3
DESCRIPTION: B1-B18
SAMPLING HEIGHT(M) 1.0
GRID SCALE (M) 500.
DATE: 26/ 7/78 TIME: 1323-1329

GRID COOR (X)	(Y)	SF6 (PPT)	GRID COOR (X)	(Y)	SF6 (PPT)
2.4	8.5	0.	7.1	5.4	0.
2.5	8.0	0.	7.3	5.2	0.
2.6	7.9	0.	7.4	4.9	0.
2.9	7.8	0.			
3.0	7.7	0.			
3.2	7.6	0.			
3.5	7.5	0.			
3.7	7.3	0.			
4.1	7.2	0.			
4.5	7.1	0.			
4.8	6.5	0.			
5.5	6.1	0.			
6.0	5.9	0.			
6.6	5.8	0.			
6.9	5.6	0.			

TEST NO. 8
DATA SET NO. 4
DESCRIPTION: B1-B13
SAMPLING HEIGHT(M) 1.0
GRID SCALE (M) 500.
DATE: 26/ 7/78 TIME: 1359-1403

GRID COOR (X)	(Y)	SF6 (PPT)
2.4	8.5	0.
2.5	8.0	0.
2.6	7.9	0.
2.9	7.8	0.
3.0	7.7	0.
3.2	7.6	0.
3.5	7.5	0.
3.7	7.3	0.
4.1	7.2	0.
4.5	7.1	0.
4.8	6.5	0.
5.5	6.1	0.
6.0	5.9	0.

TEST NO. 8
DATA SET NO. 5
DESCRIPTION: 15-MINUTE AVERAGE DATA
SAMPLING HEIGHT(M) 1.0
GRID SCALE (M) 50.
DATE: 26/ 7/78 TIME: 1315-1330

GRID COOR (X)	(Y)	SF6 (PPT)	GRID COOR (X)	(Y)	SF6 (PPT)
.8	18.4	84.	16.6	10.3	-1.
1.8	17.5	100.	17.9	8.2	35.
2.8	16.7	61.	18.9	6.1	-1.
4.0	16.1	32.	19.9	4.0	-1.
5.4	15.5	64.			
6.4	14.9	77.			
6.7	14.3	48.			
7.3	13.7	171.			
8.8	13.7	206.			
10.1	14.2	106.			
10.5	15.4	68.			
11.6	16.0	-1.			
13.6	15.4	0.			
15.9	15.3	0.			
15.6	12.8	0.			

Table A3: Cont.

TEST NO. 9
DATA SET NO. 1
DESCRIPTION: 15-MINUTE AVERAGE DATA
SAMPLING HEIGHT(M) 1.0
GRID SCALE (M) 500.
DATE: 26/ 7/78 TIME: 1630-1645

GRID COOR (X)	(Y)	SF6 (PPT)	GRID COOR (X)	(Y)	SF6 (PPT)
2.6	3.0	0.	4.2	2.2	0.
2.7	2.9	-1.	4.4	2.0	0.
2.9	2.7	0.	4.6	1.8	0.
3.0	2.7	0.	4.7	1.5	0.
3.1	2.6	0.	2.4	8.5	0.
3.2	2.6	0.	2.5	8.0	0.
3.3	2.5	0.	2.6	7.9	0.
3.4	2.5	55.	2.9	7.8	0.
3.5	2.5	116.	3.0	7.7	0.
3.6	2.6	129.	3.2	7.6	0.
3.7	2.7	158.	3.5	7.5	0.
3.8	2.8	48.	3.7	7.3	0.
4.0	2.7	16.	4.1	7.2	0.
4.	2.7	0.	4.5	7.1	0.
4.	2.4	0.	4.8	6.5	0.

TEST NO. 9
DATA SET NO. 2
DESCRIPTION: B1-B19
SAMPLING HEIGHT(M) 1.0
GRID SCALE (M) 500.
DATE: 26/ 7/78 TIME: 1627-1638

GRID COOR (X)	(Y)	SF6 (PPT)	GRID COOR (X)	(Y)	SF6 (PPT)
2.4	8.5	0.	7.1	5.4	0.
2.5	8.0	0.	7.3	5.2	0.
2.6	7.9	0.	7.4	4.9	0.
2.9	7.8	0.	7.8	4.4	0.
3.0	7.7	0.			
3.2	7.6	0.			
3.5	7.5	0.			
3.7	7.3	0.			
4.1	7.2	0.			
4.5	7.1	0.			
4.8	6.5	0.			
5.5	6.1	0.			
6.0	5.9	0.			
6.6	5.8	0.			
6.9	5.6	0.			

TEST NO. 9
DATA SET NO. 3
DESCRIPTION: B1-B19
SAMPLING HEIGHT(M) 1.0
GRID SCALE (M) 500.
DATE: 26/ 7/78 TIME: 1639-1645

GRID COOR (X)	(Y)	SF6 (PPT)	GRID COOR (X)	(Y)	SF6 (PPT)
2.4	8.5	0.	7.1	5.4	0.
2.5	8.0	0.	7.3	5.2	0.
2.6	7.9	0.	7.4	4.9	0.
2.9	7.8	0.	7.8	4.4	0.
3.0	7.7	0.			
3.2	7.6	0.			
3.5	7.5	0.			
3.7	7.3	0.			
4.1	7.2	0.			
4.5	7.1	0.			
4.8	6.5	0.			
5.5	6.1	0.			
6.0	5.9	0.			
6.6	5.8	0.			
6.9	5.6	0.			

TEST NO. 9
DATA SET NO. 5
DESCRIPTION: 15-MINUTE AVERAGE DATA
SAMPLING HEIGHT(M) 1.0
GRID SCALE (M) 50.
DATE: 26/ 7/78 TIME: 1630-1645

GRID COOR (X)	(Y)	SF6 (PPT)	GRID COOR (X)	(Y)	SF6 (PPT)
.8	18.4	0.	16.6	10.3	0.
1.8	17.5	-1.	17.9	8.2	0.
2.8	16.7	0.	18.9	6.1	0.
4.0	16.1	0.	19.9	4.0	0.
5.4	15.5	0.			
6.4	14.9	0.			
6.7	14.3	0.			
7.3	13.7	55.			
8.8	13.7	116.			
10.1	14.2	129.			
10.5	15.4	158.			
11.6	16.0	48.			
13.6	15.4	16.			
15.9	15.3	0.			
15.6	12.8	0.			

APPENDIX B

ERRORS IN ESTIMATES OF σ_Y FROM TRACER DATA.

Three major sources of error appear in the actual use of the equations (3)-(7) in this report: one is the error inherent in the data themselves; another is due to the data being for discrete points rather than for all y; and finally, due to limitation on the sampling locations, one or both edges of the plume might be chopped off (the integration cannot be carried to the limits, $-\infty$, ∞). The errors in the data cannot be reduced once the data are taken, but errors in application of the above formulas can be estimated and reduced to some extent.

The error involved in calculating the integrals is dependent upon the method used, but the error involved in chopping off the edges of the plume can be treated generally. By assuming a perfect gaussian plume and calculating the parameters from equations *(3)* - *(7)*, but with limits of integration y_a and y_b instead of $-\infty$ and $+\infty$, the following expressions result:

$$y_o' = y_o - \frac{\sigma\, e^{-\frac{1}{2}u^2}\Big|_{u_a}^{u_b}}{\sqrt{2\pi}\, P_{(u)}\Big|_{u_a}^{u_b}} \qquad (B1)$$

$$\sigma' = \sigma\left[1 - \frac{u\, e^{-\frac{1}{2}u^2}\Big|_{u_a}^{u_b}}{\sqrt{2\pi}\, P_{(u)}\Big|_{u_a}^{u_b}} - \frac{1}{2\pi}\left(\frac{e^{-\frac{1}{2}u^2}\Big|_{u_a}^{u_b}}{P_{(u)}\Big|_{u_a}^{u_b}}\right)^2\right]^{\frac{1}{2}} \qquad (B2)$$

where

$$u = \left(\frac{Y-Y_o}{\sigma}\right) \qquad (B3)$$

and

$$P_{(u)} = \frac{1}{\sqrt{2\pi}} \int_{-\infty}^{u} e^{-\frac{1}{2}r^2}\, dr \qquad (B4)$$

(note $P_{(u)}$ is the normal probability function)

where σ and y_o are the actual parameters of the plume, and σ' and Y_o' are the parameters calculated using formulas *(3)-(7)* with limits of integration Y_a and Y_b. No simple expressions for Y_o and σ in terms of Y_o' and σ' could be found. However, equations *B1)* and *(B2)* can be applied in an iterative manner so that successively better approximations of Y_o and σ can be found as follows:

$$Y_{o(n+1)} = Y_{o(o)} + \frac{\sigma(n)\, e^{-\frac{1}{2}u^2}\Big|_{ua(n)}^{ub(n)}}{\sqrt{2\pi}\, P_{(u)}\Big|_{ua(n)}^{ub(n)}} \qquad (B5)$$

$$\sigma_{(n+1)} = \sigma_{(o)}\left[1 - \frac{u\, e^{-\frac{1}{2}u^2}\Big|_{ua(n)}^{ub(n)}}{\sqrt{2\pi}\, P_{(u)}\Big|_{ua(n)}^{ub(n)}} - \frac{1}{2\pi}\left(\frac{e^{-\frac{1}{2}u^2}\Big|_{ua(n)}^{ub(n)}}{P_{(u)}\Big|_{ua(n)}^{ub(n)}}\right)^2\right]^{-\frac{1}{2}} \qquad (B6)$$

$$U_{n(n)} = \left(\frac{Y_y - Y_{o(n)}}{\sigma_n}\right) \qquad (B7)$$

where the small subscript in parentheses refers to the number of times the interation was performed to arrive at the approximation, and (o) refer to initially calculated values. Integrals were determined using triangular approximation.

NORSK INSTITUTT FOR LUFTFORSKNING
(NORGES TEKNISK-NATURVITENSKAPELIGE FORSKNINGSRÅD)
POSTBOKS 130, 2001 LILLESTRØM
ELVEGT. 52.
TLF. (02) 71 41 70

RAPPORTTYPE	RAPPORTNR.	ISBN--82-7247- 088-8
Teknisk notat	12/78	
DATO	ANSV.SIGN.	ANT.SIDER OG BILAG
Desember 1978	O.F.Skogvold	77 2

TITTEL
Atmospheric Dispersion Experiments using the NILU automatic weather station and SF_6 tracer techniques

PROSJEKTLEDER
B.Lamb, B.Sivertsen

NILU PROSJEKT NR
2577

FORFATTER(E)
Brian Lamb
Bjarne Sivertsen

TILGJENGELIGHET **
A

OPPDRAGSGIVERS REF.

OPPDRAGSGIVER
NILU

3 STIKKORD (á maks.20 anslag)

Spredningsmodell	sporstoffteknikk	turbulensdata

REFERAT (maks. 300 anslag, 5-10 linjer)
Rapporten beskriver NILUs automatiske værstasjon (AWS), samt NILUs utstyr for sporstoffundersøkelser. Den presenterer resultatene fra spredningsforsøk for å finne sammenhengen mellom spredningsparametre til gaussmodeller og turbulens målt med AWS. Det er etablert en sammenheng mellom horisontal vindfluktuasjon (σ_θ) og horisontal konsentrasjonsfordeling (σ_y). Tilsvarende forhold er forsøkt etablert mellom vertikale vind- og temperatur profiler og vertikal konsentrasjonsfordeling σ_z.

TITTEL

ABSTRACT (max. 300 characters, 5-10 lines)
A description of the NILU automatic weather station (AWS) and the SF_6-tracer equipment is presented. Dispersionexperiments are described to establish the relationship between horizontal wind fluctuation measurements (σ_θ) and σ_y, and between vertical wind and temperaturprofile data and σ_z.

**Kategorier: Åpen - kan bestilles fra NILU A
Må bestilles gjennom oppdragsgiver B
Kan ikke utleveres C